NON-COVALENT INTERACTIONS OF TRIMETHYLAMINE N-OXIDE (TMAO) AND UREA IN WATER

John Caswell Prather

A thesis submitted to the faculty of The University of Mississippi in partial fulfillment of the requirements of the Sally McDonnell Barksdale Honors College

University of Mississippi

May 2015

Approved by

_____

Advisor: Professor Nathan Hammer

_____

Reader: Professor Gregory Tschumper

_____

Reader: Professor Susan Pedigo

ABSTRACT

TMAO and urea are important osmolytes. Osmolytes help maintain cell volume with their presence inside and outside cells. Urea is used by kidney cells to neutralize strong osmotic gradients caused by excretion of hypertonic waste. Although urea is for volume-maintaining purposes, it is also known to be a strong denaturant of cellular proteins. The method by which urea destabilizes folded proteins is a debated topic. There is evidence that urea binds directly to amino acid side chains to make protein folding less thermodynamically favored. It has also been suggested that urea acts indirectly to denature proteins by destabilizing the surrounding hydrogen bonding water networks. The destabilized network allows free water molecules to interact with polar protein side chains. This indirect method is similar to the suggested method by which TMAO acts as a protein stabilizer. TMAO has been shown to counteract urea denaturation of proteins, when both are present in the cell. The mechanism for this counteraction is investigated in this project. Experimental Raman spectra of saturated urea, saturated TMAO, and saturated TMAO-urea solutions are obtained using a scanning Raman spectrometer. Theoretical calculations are performed to obtain optimized structures and simulated vibrational frequencies and Raman intensities. Experimental data shows that the addition of TMAO into a solution of saturated urea causes an 11 cm^{-1} blue shift of the HNH urea symmetric bending mode. This experimental shift is reproduced theoretically.

ACKNOWLEDGEMENTS

I would like to thank Dr. Hammer for his support throughout my project and for challenging me to become a better student and a self-motivated worker. I would like to thank John Kelly for his insight and suggestions to my project. I would also like to thank Dr. Tschumper and Dr. Pedigo for being on my committee and dealing with my extreme procrastination.

TABLE OF CONTENTS

CHAPTER 1: NON-COVALENT INTERACTIONS AND THE HYDROPHOBIC EFFECT

A covalent bond is an interaction between two atoms that involves each atom sharing one or more of its valence electrons with the other atom. Although a covalent bond's sharing of valence electrons allows for the building of molecules from single atoms, it is not the only interaction that is vitally important to nature. Non-covalent interactions are interactions that are weaker than covalent interactions and that do not involve sharing electrons. These interactions can occur between intermolecular atoms, from different molecules, or intramolecular atoms, from the same molecule. Although each individual non-covalent interaction is much weaker than a covalent interaction, non-covalent interactions can grow very strong when they occur in large quantities, such as hydrogen bonding interactions that contribute to proteins' folded structures.[1] The many types of non-covalent interactions include ionic interactions, halogen bonding, ion-dipole interactions, dipole-dipole interactions, and van der Waals forces. The important non-covalent interaction of this study is hydrogen bonding, a special type of dipole-dipole interaction.

1.1 Hydrogen Bonding

The hydrogen bond is one of the most important chemical phenomena in nature. Hydrogen bonding is the reason that water has a higher boiling point than any other covalent hydride molecule, and it is responsible for strengthening protein and nucleic acid structures. The hydrogen bond arises from an electrostatic attraction between an "electron deficient" hydrogen atom (H) that is bound to a highly electronegative atom (O,

N, or F) and a nearby "electron-dense" (electronegative) atom or region (O, N, or F). The formal definition of a hydrogen bond, defined by the IUPAC Task Group, is "an attractive interaction between the hydrogen from a group X—H and an atom or group of atoms Y, in the same or different molecule(s), where there is evidence of a partial bond formation".[2] The hydrogen bonds of particular interest in this work are water-water hydrogen bonds, water-urea hydrogen bonds, water-TMAO hydrogen bonds, and TMAO-urea interactions (examples shown in Figure 1.1.1).

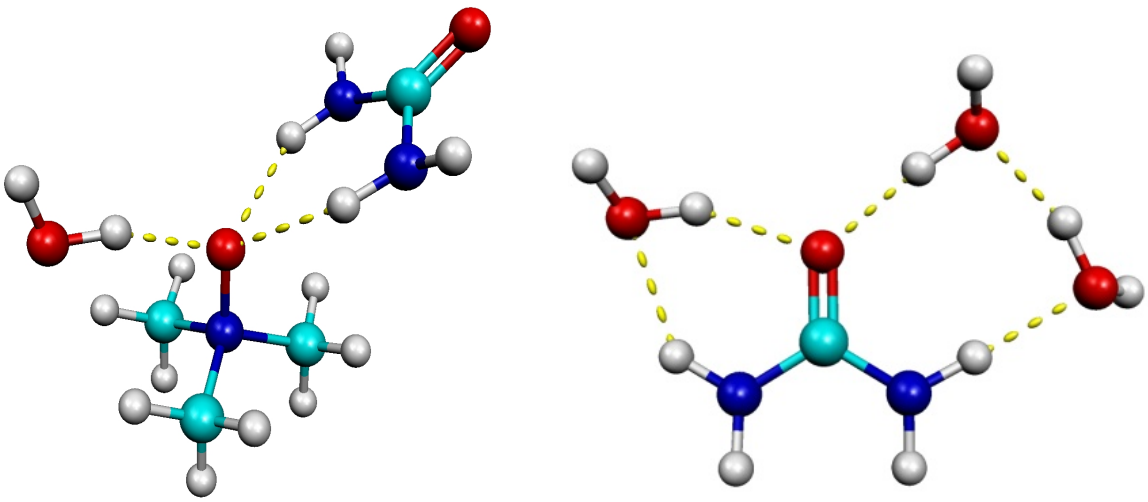

Figure 1.1.1: (Left) Water-TMAO and TMAO-Urea Hydrogen Bonds; (Right) Water-Urea Hydrogen Bonds

When describing hydrogen bonds, the terms "hydrogen-bond donor" and hydrogen-bond acceptor" are used. The hydrogen-bond donor is the molecule/atom that is covalently bonded to the hydrogen (X---H). The hydrogen-bond acceptor is the electronegative region/atom that is attracted to the partial positively charged hydrogen atom. Thus, in the left image of Figure 1.1.1, TMAO is the hydrogen-bond acceptor in all hydrogen bonds, and water and urea are hydrogen-bond donors. On the right, however, urea is "accepting" hydrogen bonds from the waters. It is important to understand that the hydrogen atom is neither accepted nor donated during hydrogen bonding interactions.

Instead, the hydrogen bond is an electrostatic attraction between partial positive and electronegative atoms. Hydrogen bonds between water molecules are very important to biological processes. Water molecules are known to hydrogen bond between themselves to form extended hydrogen-bonding networks.[3-4] Networks of water molecules, bound by hydrogen bonds, influence many biological processes including solvating hydrophobic groups in macromolecules, such as proteins, and interacting with or excluding hydrophilic groups on protein backbones. Furthermore, small biological molecules, such as urea and TMAO, can have a profound impact on biological processes by hydrogen bonding with the water networks. These interactions are discussed in Chapter 2, and the effect of osmolyte-water interactions on extended water networks is a topic of interest in this paper and in previous group members' research.[4]

1.2 The Hydrophobic Effect

The hydrophobic effect is sometimes referred to as a non-covalent interaction. It might be convenient to describe the hydrophobic effect as an attractive interaction between two or more hydrophobic molecules, but the actual mechanism behind the hydrophobic effect should be viewed as both enthalpic and entropic.[5] The Gibbs Free Energy (ΔG) is a thermodynamic term to describe the potential usefulness of a system. When discussing the hydrophobic effect (especially pertaining to protein folding), it is important to note that the solute/solvent system interactions will act to minimize the Gibbs Free Energy of that system. Both enthalpy and entropy affect the Gibbs Free Energy, as seen in Equation 1.1:

$$\Delta G=\Delta H-T\Delta S \qquad 1.1$$

Where ΔG is change in Gibbs Free Energy, ΔH is change in enthalpy, T is temperature and ΔS is change in entropy of the system. Thus, the hydrophobic effect is caused by the system forming hydrogen bonds to minimize the enthalpy and maximizing entropy by decreasing the order of the system.

Water molecules prefer to form hydrogen bonds with themselves in solution. Thus, when a solute is placed in aqueous solution, water-water hydrogen bonds are broken to make space for new molecules. If the new molecules can form hydrogen bonds with water molecules (hydrophilic), the solute molecules are dispersed throughout the solution, interacting with as many water molecules as possible. If the solutes are hydrophobic, however, the broken hydrogen bonds between water molecules cannot be replaced by solute-water hydrogen bonds. At most, hydrophobic molecules will interact with water through dipole induced-dipole interactions, which are much weaker than hydrogen bonds. Instead of water-solute interactions, water-water hydrogen bonds are strengthened around the hydrophobic molecule by each water molecule interacting with four other waters. Although this strengthening of hydrogen bonds would account for the loss of enthalpy caused by the hydrophobic molecule, the water molecules around the hydrophobic molecule are left in a highly ordered ice-like network that is sometimes referred to as a solvation shell or cage. The highly ordered water "cages" created by the addition of hydrophobic molecules is unfavorable due to the decrease in entropy. Thus, hydrophobic molecules tend to clump together in aqueous solution to minimize the amount of water "cages" needed for their solvation. This clumping together to maximize entropy is entropic contribution to the hydrophobic effect.[5]

The hydrophobic effect plays a role in many cellular processes. It is responsible for a lipid bilayer membrane's formation and semi-permeability. The lipid bilayer consists of an outside layer of hydrophilic lipid heads, surrounding an inside layer of hydrophobic lipid tails.[6] Another biological process that utilizes the hydrophobic effect is protein folding. Proteins are macromolecules constructed with long chains of amino acids. At pH seven, there are nine amino acids with hydrophobic side chains and six amino acids with hydrophilic side chains.[7] Therefore, almost every protein is going to contain several hydrophobic and hydrophilic amino acids. The hydrophobic effect is the driving force behind the amino acid chain being folded into its native and functional protein form. As discussed above, the amino acids containing hydrophilic side chains will easily interact with aqueous solution, replacing any destroyed water-water hydrogen bonds with side chain-water hydrogen bonds. Several of these hydrophilic amino acids will remain on the outside surface of the folded protein. The amino acids with hydrophobic side chains, however, will aggregate together to minimize the need for rigid ice-like water networks surrounding them. These hydrophobic amino acids are said to "bury" themselves inside the folded protein. In addition, other hydrophilic amino acid side chains will interact together inside of the folded protein to further stabilize the folded structure. In this way, hydrogen bonding and the hydrophobic effect can drive the formation of functional folded proteins.

The lowest energy, folded protein structure is the protein structure that allows for proper function by the protein, and the structure is termed the native state. The hydrophobic effect drive the protein structure down in energy until it reaches a minimum energy, where most hydrophobic groups are "buried" inside the protein. This exothermic

process creates a highly ordered product (the native protein), resulting in a loss in entropy. The reason that protein folding is still spontaneous is that the entropy lost in the ordering of the folded protein is outweighed by the entropy gained in avoiding wide spread ordering of water cages around the protein hydrophobic sites.[8]

Osmolytes, such as TMAO and urea, act to destabilize or stabilize proteins. The mechanism that TMAO and urea employ to influence the protein stability is still under debate, but one of the proposed hypotheses is that TMAO and urea act indirectly, through the water hydrogen bonding networks. The osmolyte might interact with the surrounding hydrogen bonding network of water to increase the strength and rigidity of the network (TMAO), making it even more favorable for the protein to stay in its folded state (minimal hydrophobic-water interaction). Urea, on the other hand, might weaken the hydrogen-bonding network surrounding proteins, making it less costly for hydrophobic groups to be in contact with water molecules. The details of the indirect mechanism are discussed in more detail in Chapter 2.

CHAPTER 2: OSMOLYTES

Osmolytes are small organic molecules, present inside cells of nearly all living organisms including bacteria, plants and animals.[2] These small molecules are vital to regulating cell volume, and protect proteins' stability in water-stressed environments. All osmolytes, with the exception of urea, are "compatible solutes" that do not perturb cellular macromolecules even in high concentrations.[9] This characteristic of osmolytes is a clear advantage over other water-regulating mechanisms such as inorganic salt accumulation in mammalian cells, which can be harmful to cellular function in high concentrations.[2] Specifically, osmolytes are known to be used by mammalian renal medulla cells to maintain cell volume in the presence of the kidney's extremely high hypertonic environment.[10] Other than urea, protecting osmolytes are classified into three groups: (1) Polyols, which include glycerol, sucrose and other sugars; (2) amino acids like proline and glycine; (3) and methylamines such as sarcosine and trimethylamine N-oxide (TMAO).[10] TMAO is often seen in urea-rich cells because TMAO prevents the deleterious effects of urea. The interactions of TMAO and urea in water are the main focus of this study.

2.1 TMAO as an Osmolyte

Trimethylamine N-oxide (TMAO) is a methylamine whose structure is shown in Figure 2.1.1 TMAO is one of the most studied osmolytes, and it is known that TMAO stabilizes protein structure. However, there has been much debate about exactly how

TMAO affects protein stability, and relatively little is known about the possible mechanisms that are used.

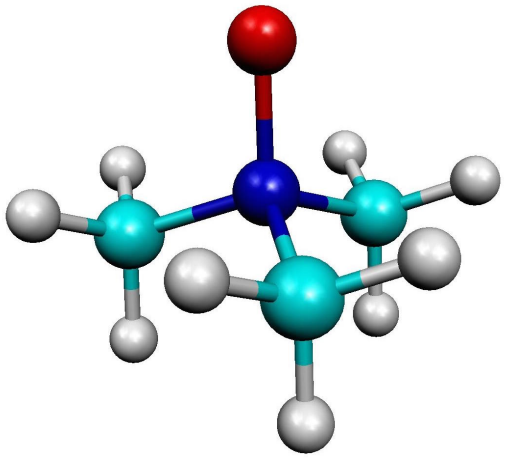

Figure 2.1.1: Structure of trimethylamine N-oxide (TMAO)

There are two dominating hypotheses on how TMAO (and other osmolytes) might interact with proteins: by directly binding to the protein (direct method) or by indirectly interacting with the solvent surrounding the protein (indirect method). Although some studies suggest that solvent interactions do not play a large role in protein stabilization by TMAO, many recent studies have argued that the major mechanism used by TMAO to stabilize proteins is indirect, through non-covalent interactions with surrounding solvent.[3-4, 11] TMAO/water interactions create a stronger water-water hydrogen bonding network than pure water, which "dehydrates" the area around the protein backbone carbonyl group.[3] This increase in entropy surrounding the protein makes the unfolded protein structure even more unfavorable. One reason that the indirect method has been favored over the direct method for TMAO is that investigators have shown that TMAO is preferentially excluded from interacting with the protein backbone and side chain units of proteins, causing a destabilization of the unfolded protein

structure[12]. This exclusion from backbone interaction, coupled with the fact that TMAO molecules take up space around the proteins, suggests that there is likely another mechanism by which TMAO affects protein stability, called the excluded volume effect. TMAO molecules take up space around the protein, which causes a shift in the thermodynamic equilibrium between unfolded and folded protein states. The folded protein structure, which has less surface area, becomes more favorable with less available space due to TMAO's presence.[12-14] Thus, TMAO 's strong hydrogen bonding with water around proteins minimizes solvation shell-protein hydrogen bonding, and TMAO is excluded from the protein backbone, leading to a decrease in the favorability of the unfolded state of the protein.[14]

2.2 Urea as an Osmolyte

Urea ($(NH_2)_2$ CO) is an organic molecule that is found in a wide variety of living organisms. Its structure is shown in Figure 2.2.2. In humans, urea is formed in the liver. Ammonia, which builds up as waste from amino acid breakdown, is an extremely toxic base. The liver quickly creates urea from two ammonia molecules and one carbon dioxide molecule to remove ammonia. Mammals excrete urea in urine as nitrogenous waste, but, in order to excrete highly concentrated urine and reabsorb water, urea is also used as an osmolyte. Inside nephrons, loops of Henle are used to concentrate urine before it is excreted. The loop of Henle takes the filtrate through the inner medulla of the kidney, which contains cells that are hypertonic compared to the filtrate. This osmotic gradient allows water to diffuse out of the filtrate and back into the kidney, concentrating the urea in the filtrate (urine). Although urea is being excreted in this process, it also is a solute

that is used by the cells in the inner medulla to remain hypertonic to the filtrate. Thus, urea helps to maintain the hypertonic osmolarity of cells in the kidney.

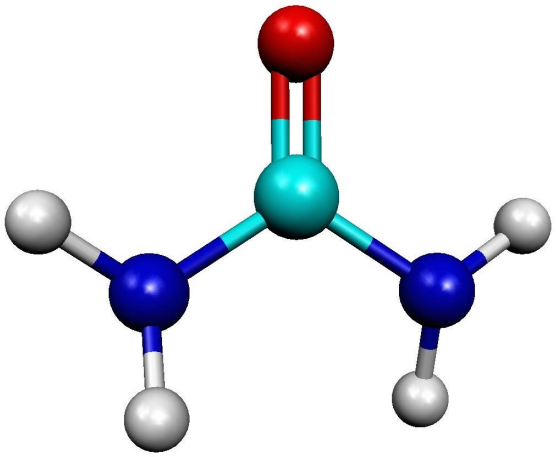

Figure 2.2.2: Structure of urea

As mentioned above, urea destabilizes proteins. The question of whether urea destabilization occurs in a direct or indirect manner has not been fully answered. The study of urea/water step-by-step denaturing of proteins by Wei shows that water is the attacking molecule on the amide C=O group that breaks protein hydrogen bonds[3]. The results of this study suggest that urea's role in the destabilization of proteins is its influence on water-water interactions that promote water-protein hydrogen bonding. Furthermore, this study showed that although water, promoted by urea, is the more favorable hydrogen-bonding agent with the protein backbone. Urea also hydrogen bonds to C=O groups on the protein backbone. This suggests that, unlike TMAO, urea is likely to denature proteins by both the indirect and direct method. Somewhat contrary to the previous studies findings are the findings of a study in 2009 involving analysis of the effects of TMAO and urea on secondary structure of hen egg white lysozyme. This study

found that low concentrations of urea lacked the ability to strengthen or weaken the water hydrogen-bonding network like TMAO. However, in higher concentrations, urea bonded with the protein's backbone, weakening surrounding waters' hydrophobic effect and destabilizing the protein[15]. Another study by Hua and Zhou supports this hypothesis. In this study, a molecular mechanism for direct urea denaturation is presented. It is shown that, because urea has stronger Van der Waals dispersion interactions with the protein than urea does, urea displaces water in the protein solvation shell, and hydrogen bonds tightly with the protein backbone in a two-step process. Finally, it has been suggested that urea's interactions with water promotes the solvation of hydrophobic groups in the unfolded state of proteins, but urea also hydrogen bonds directly to the backbone of proteins[16]. As these studies show, a clear consensus on the mechanism for urea's denaturing effects has not yet been reached. Urea, in high concentrations, clearly interacts directly with proteins, but the extent of indirect effect through water interaction has yet to be clearly determined.

2.3 TMAO Counteracts Urea's Denaturing Effects

When both urea and TMAO are present in the cell, TMAO counteracts urea's denaturing effects on proteins. Thus, TMAO not only stabilizes folded proteins, it plays the vital role of protein protector for urea-rich cells. It has been established that only a 1:2 TMAO to urea concentration ratio is needed for TMAO to effectively counteract urea's denaturation.[16-18] Although the counteraction by TMAO is evident, the mechanism by which the counteraction happens has not been discovered. The hypothesis that TMAO's stabilization of the folded protein state overpowers the stabilization of the unfolded

protein state by urea has been presented by Qu, Wang and Bolen.[17-18] In Qu and Bolen's study, hydrogen exchange rates were examined at different amide groups on RNase A, a RNA-cleaving enzyme found in the cell. Because amide groups in a tightly folded protein will be compacted and often hydrogen bonded, there is little to no protein exchange. In a less compact unfolded state, amide protons will see an increase in proton exchange. It was argued that TMAO constricts amide proton exchange through its unfavorable reactions with the side chains of proteins. In contrast, urea expands the protein structure by increasing amide proton exchange rate and amplitude through its favorable interaction with protein side chains. Qu and Bolen found that TMAO was able to affect exchange rates of urea effected exchange sites along with other sites that urea did not change. It was hypothesized that TMAO's ability to affect more exchange sites attributes to its ability to counteract urea denaturation.[18] Furthermore, Wang and Bolen examined urea and TMAO effects by analyzing transfer free energy measurements. They argued that favorable TMAO interaction with protein side-chains actually promotes protein denaturation; however, the highly unfavorable TMAO peptide-backbone interaction more than offsets the favorable TMAO side-chain interaction. Urea interacts favorably with both the protein peptide backbone and protein side chains. As evidence that urea and TMAO both favorably interact with protein side chains to stabilize the unfolded state, it was shown that a solution of TMAO and urea actually increased the contributions of side chains in protein unfolding. Because TMAO and urea both contribute to unfolding at the side chain sites any, TMAO protection against denaturation must come, solely, from the unfavorable TMAO-peptide backbone contributions. The unfavorable TMAO-peptide backbone interactions essentially mean that TMAO exclusion from the surface of

proteins is highly favorable; this leads to preferential hydration of the protein instead of TMAO interaction. The authors argue that the proposed mechanism makes sense because TMAO has the ability to counteract urea-denaturing effects in all proteins. If the source of TMAO protection came from side chain interactions, the effectiveness of the protection would be dependent upon the side chain content of different proteins, which is highly variable from protein to protein. Instead, TMAO's exclusion effect on peptide backbones allows it to effectively nullify urea denaturation in all proteins.[17] These two studies have highlighted the hypothesis that TMAO's stabilization of the folded protein structure overpowers urea's stabilization of the unfolded protein structure, by either affecting more exchange sites or through the more powerful TMAO exclusion from protein surfaces.[17-18] One hypothesis that has not been fully investigated is that TMAO counteraction is due to TMAO and urea interacting together in solution. One study, conducted in 2010, concluded that TMAO's oxygen preferentially interacts with urea's amine groups over water, when TMAO and urea are in solution. The argument is that this direct TMAO-urea interaction, coupled with TMAO's exclusion effect, accounts for the ability of TMAO to counteract urea denaturation in solutions of 1:2 TMAO-urea concentration ratio, regardless of urea concentration.[19] Finally, renal medulla cells are estimated to contain about 0.5 mol L^{-1} urea and 0.2 mol L^{-1} TMAO.[9] A molecular basis for TMAO interacting with urea in solution is investigated in this project.

CHAPTER 3: SPECTROSCOPIC AND THEORETICAL METHODS

Two important chemistry techniques are employed in this experiment to study hydrogen bonding between TMAO, urea and water. First, spectroscopy is used to gather experimental data on TMAO-urea-water interactions. Second, computational chemistry helps predict the molecular level interactions using first principles to solve the Schrödinger equation.

3.1 Spectroscopy

Spectroscopy is the study of electromagnetic radiation and matter interactions. Although the human eye can detect electromagnetic radiation in the energy range of visible light, most radiant energies are not visible to the human eye. All radiant energies of the electromagnetic spectrum, shown in Figure 3.1.1, interact differently with matter. The discovery that electromagnetic radiation has "wave-particle duality", having characteristics of both a wave and a particle, is one of the most important and baffling discoveries in science.[20] In some cases, it is convenient to view light as a wave. For instance, the wave frequency (υ) of light is the number of crests passing a fixed point per second, and the wavelength (λ) of light is the distance between two adjacent crests in a light wave. Frequency and wavelength are related by the equation $c= \lambda\upsilon$, where c is the speed of light in a vacuum. These two wave characteristics are often used to quantify energy in the electromagnetic spectrum, because each relates to electromagnetic radiation energy by the equation $E=h\upsilon$ or $E=\frac{hc}{\lambda}$. Therefore, frequency is a unit that is directly proportional to energy, and wavelength is a unit that is inversely proportional to energy. At other times, light is viewed as a particle, called a photon. It is convenient to view light

as a particle when studying how light interacts with matter. Matter can interact with a photon of light, with energy hυ, in myriads of ways, but some of the most common interactions are absorption, scattering, emission, and reflection.[20] At this point in the understanding of spectroscopy, it is important to view light-matter interactions from the matter perspective.

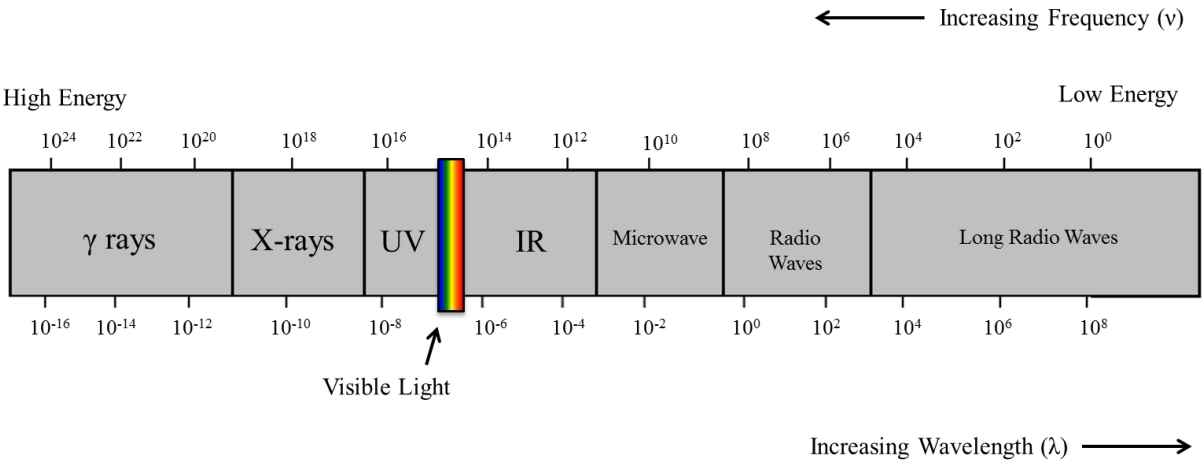

Figure 3.1.1: Electromagnetic Spectrum

Molecules and free atoms are always in constant motion. Molecules and atoms can be in the gas phase, where individual molecules, or atoms, are widely separated from each other. They can also be in the liquid phase, where there is more interaction between molecules, or they can be tightly packed into a solid phase.[20] No matter what phase molecules and atoms are in, however, they are always in constant motion. Molecules vibrate, rotate or translate (a movement from one place to another). Individual atoms cannot rotate or vibrate, but they can translate through space. Their electrons can also move between electronic energy levels. It is through these motions that light interacts with matter. The energy of bond vibrations, bond rotations and electron movement in atoms can be illustrated using energy levels. For instance, a normal vibrational frequency of a bond between two atoms in a molecule can be viewed as the ground state vibrational

level. In quantum mechanics, an increase in the vibrational frequency of that bond would correspond to a transition from the ground vibrational level to an excited vibrational level. The same holds true for rotation energies, although a rotational transition requires much less energy. For electronic transitions in atoms, an electron can be excited from a ground state energy level to an excited energy state.[21] Transitions between vibrational and rotational sublevels and an electronic transition are shown in Figure 3.1.2. Raman stokes line, which is also shown, will be discussed later.

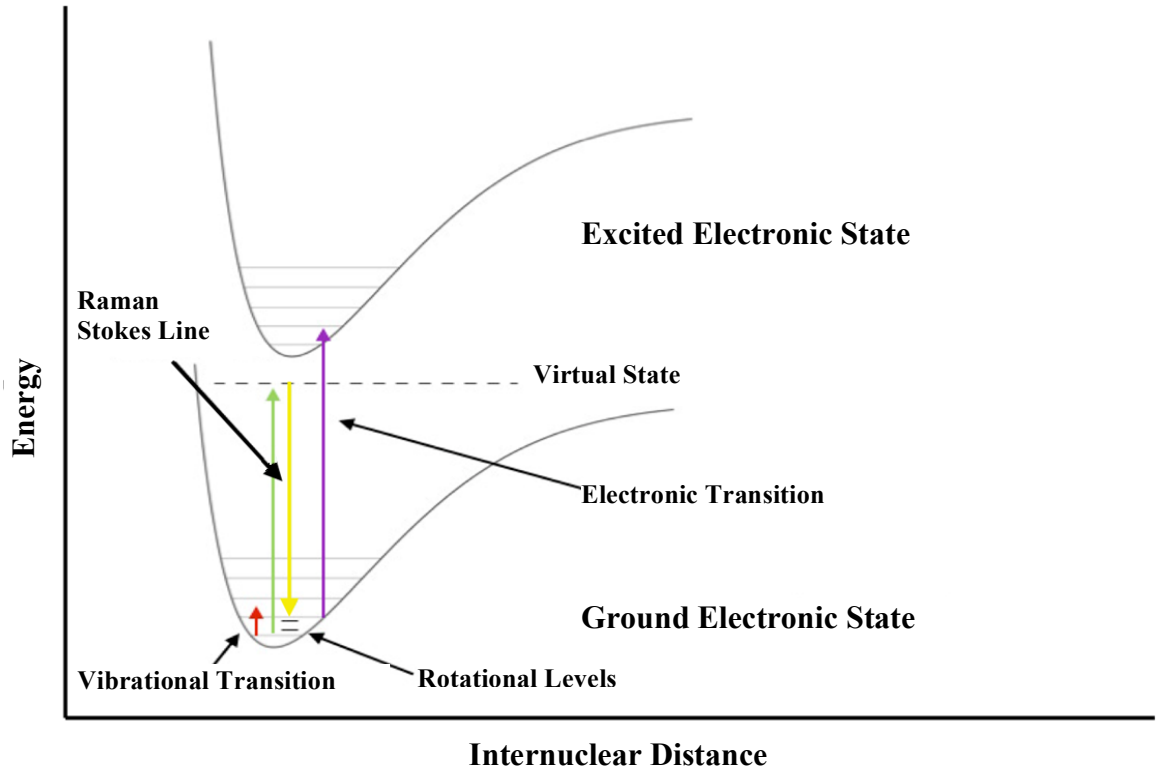

Figure 3.1.2: Vibrational, Rotational, and Electronic Transitions; The Raman stokes line

Photons interact with matter by causing an increase in energy, or decrease in the case of emission, in these motions. The unique feature that makes spectroscopy such an effective tool for studying molecules is that molecules will only absorb photons whose energy exactly matches the change in energy between two energy levels, and there are

specific radiation energy ranges that will interact with certain molecular processes (vibrational, rotational and electronic transitions).

Vibrational spectroscopy, specifically Raman spectroscopy, is used in this project. The radiation frequency that matches vibrational transition frequency is infrared (IR) light. Vibrational spectroscopy is a useful tool in analyzing molecules because: (1) the vibrational frequency of a bond depends almost completely on the two attached atoms, not the surrounding atoms, and (2) a given bond (also called a vibrational mode) only has one intense frequency.[21] These two characteristics are oversimplified for larger molecules or systems because vibrational modes will often couple at a given frequency in larger systems. This second feature of vibrational modes is due to the fact that it is exponentially more probable that a diatomic molecule (or any bond in a molecule) will be found at the ground vibrational level as opposed to the first excited vibrational level. The Boltzmann distribution gives an approximation of the fraction of molecules in the ground vibrational level for a given normal mode:

$$\frac{N_1}{N_0} = \frac{g_1}{g_0} e^{-\Delta E / k_B T}$$

3.1

Where N_1/N_0 is the ratio of excited vibrational state to ground excited state, g_1/g_0 is the degeneracies of the energy levels, ΔE is the change in energy between vibrational levels, T is temperature, and k_B is Boltzmann's constant or 1.38×10^{-23} J/K. At room temperature, this equation yields an extremely small number, showing that the vast majority of vibrational modes are in their ground vibrational state. Thus, each vibrational mode contains one intense vibrational transition that will occur when a unique light wavelength is absorbed by the molecule.

3.2 Raman Spectroscopy

Raman spectroscopy, a unique type of vibrational spectroscopy, was used in this project. Raman spectroscopy uses light scattering instead of light absorption to evaluate molecular vibrations. IR spectroscopy requires a change in dipole moment upon vibration of a mode in order for light to be absorbed. Raman spectroscopy's selection rule, however, only requires that the mode change the polarizability of the bond. Even if there is no change in separation of opposite charges (change in dipole moment), a vibration might distort the electron cloud around that bond. Distortion of the electron cloud becomes easier with bond lengthening, and it becomes harder as the bond shortens. This distortion of electron density is a change in bond polarizability.[20] Some bond vibrations change the polarizability but no the dipole moment, or vice versa. In this way, IR spectroscopy and Raman spectroscopy can be used as complementary techniques. As mentioned above, Raman spectroscopy uses scattered light instead of absorbed light to evaluate molecular vibrations. When light is passed through a molecule, some radiation is scattered, and the energy of this scattered light can be used to study molecular vibrations. There are three types of light scattering: Rayleigh scattering, Stokes scattering, and Anti-Stokes scattering. The vast majority of photons scatter with the same energy that they had before collision with a molecule. In other words, the bond is excited, briefly, to an excited vibrational energy level before relaxing back to the ground vibrational level. This type of scattering, where no energy is lost, is called Rayleigh scattering, and it occurs from an elastic collision between photon and molecule. However, about one in every million interactions will result in a photon being scattered with less energy than the

incident radiation. This type of scattering, called Stokes scattering, involves inelastic collisions between photon and molecule that temporarily excites the bond to a virtual energy level before it relaxes to an excited vibrational level. Thus, the photon that is scattered leaves with energy having been lost to the molecule. This is the type of Raman scattering that is most often utilized for spectroscopy.[20] Finally, when the scattered light has greater energy than it did before the collision, the molecule will relax to a lower vibrational energy level after temporary excitation to a virtual state. This type of inelastic scattering is known as anti-Stokes scattering, and it is an extremely rare phenomenon. In order for anti-Stokes lines to be viewed, the molecules must be heated so that a

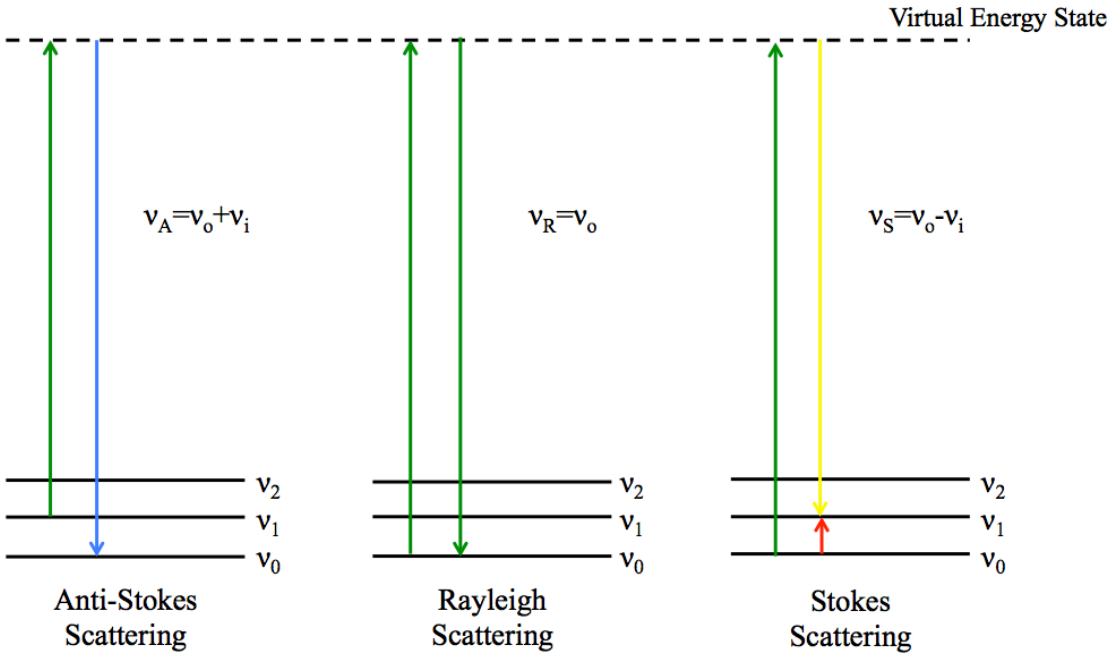

Figure 3.2.1: Types of Raman Scattering

substantial amount of vibrational modes will be found in an excited vibrational state before the collision (see Boltzmann's distribution). A diagram of all three scattering lines is shown in Figure 3.1.1.

In Raman spectroscopy, a laser is usually used as the light source. The incident light travels through a series of mirrors, and it collides with the molecules of sample in the sample cell. Then, the light scattered at 90 degrees from the incident light entry slit travels into the scanning spectrometer. The spectrometer sequentially allows single wavelengths of light to pass into the detector. The details of the Raman spectroscopy methods used in this experiment will be discussed in Section 3.4.

3.3 Computational Chemistry

Computational chemistry has quickly become a powerful tool for observing and confirming chemical mechanisms occurring at the molecular level. Computational chemistry programs use quantum mechanical theories to find theoretical values such as vibrational frequencies, optimal molecular geometries, or zero-point energies.[21]

In order to use computational chemistry to analyze light-matter interactions, the many energy levels of molecules must be determined. This is done using the time-independent Schrödinger equation:

$$\hat{H}\psi = E\psi \qquad 3.2$$

Where $\hat{H}$ is the Hamiltonian, or total energy operator, ψ is the wavefunction, which describes the state of the molecule in three dimensions and E is the energy of the system. For a single electron system, such as H_2, the Schrödinger equation for the single electron and two nuclei can be solved exactly. For larger atoms and molecules with more than one electron complete determination of the Schrödinger equations is impossible, and approximations must be used to estimate the Schrödinger equation.

Calculations involving many-electron systems use the Born-Oppenheimer approximation to find the electronic Schrödinger equation of the system. In the Born-Oppenheimer approximation, electron and nuclei motions are treated separately:

$$\Psi_{total} = \Psi_{electrons} \times \Psi_{nuclei} \quad 3.3$$

The approximation can be applied accurately because of the difference in mass between nuclei and electrons. Because nuclei are much larger than electrons, nuclei are assumed to be fixed in space compared to the infinitesimal electrons that quickly move around the nuclei coordinate. Nuclei are given individual sets of Cartesian coordinates, and the electronic Schrödinger equation is solved.

The electronic Schrödinger equation cannot be solved completely in multi electron systems, because the electronic wave function cannot be fully calculated. In order to obtain the electronic Schrödinger equation, wave functions are represented as basis functions so that the Schrödinger equation can be solved algebraically. The basis functions used to approximate molecular orbitals of single electrons are usually Gaussian functions. Then, many electron wavefunctions are represented as linear combination of molecular orbitals. For any given molecular orbital, two electrons cannot have the same spin (Paul-Exclusion Principle). Because of this, linear combinations of molecular orbitals must not contain wavefunctions that describe orbitals with two same spin electrons. Using Slater determinants to describe wavefunctions satisfies the Pauli-Exclusion Principle, because Slater determinants make the wavefunction antisymmetric. The Slater determinant for a two-electron combination is shown in Equation 3.4:

$$\psi(x_1, x_2) = \frac{1}{\sqrt{2}} \begin{vmatrix} \chi_1(x_1) & \chi_2(x_1) \\ \chi_1(x_2) & \chi_2(x_2) \end{vmatrix} \quad 3.4$$

The result of this determinant is zero for any wavefunction that contains electrons with the same spin. As electrons and orbitals of a system increases, the number of determinants needed to combine wavefunction becomes enormous. Therefore, in most computations, only a subset of Slater determinants is used to determine the electronic wavefunction.

Finally, when multi electron molecules are computed, electron correlation must be accounted for in determining the energy of the molecule. In Hartree-Fock methods, electron repulsion energy is accounted for by assuming that a single electron feels the repulsion of the average of all other electrons. This average electron field acting on an electron leads to an overestimation of electron repulsion. Therefore, other methods use more complex computations to find lower energy electron correlation energies.[22]

The B3LYP method, a Density Functional Theory (DFT) method, is used for computations in this project. DFT methods first compute the energy of a molecule using the Hartree-Fock electron correlation estimation. After the Hartree-Fock computation, DFT uses functionals of spatially dependent electron density to lower the overestimated electron correlation.[22]

Basis sets, as discussed above, are sets of Gaussian basis functions that are linearly combined to describe molecular orbitals. Larger basis sets will contain more functions, and will yield more accurate approximations of molecular orbitals. However, larger basis sets will take more computing power and more time. A rather large basis set was used in this project. 6-311++g(2df,2pd) triple zeta basis set contains 226 basis functions.

3.4 Experimental and Theoretical Methods

Experimental Raman spectra were gathered using a Jobin-Yvon Ramanor HG2-S scanning Raman spectrometer. Molecules were excited with the 514.5 nm laser line of a SpectraPhysics Kr+/Ar+ laser. A schematic of our lab's Raman spectroscopy set up is shown in Figure 3.4.1.[23]

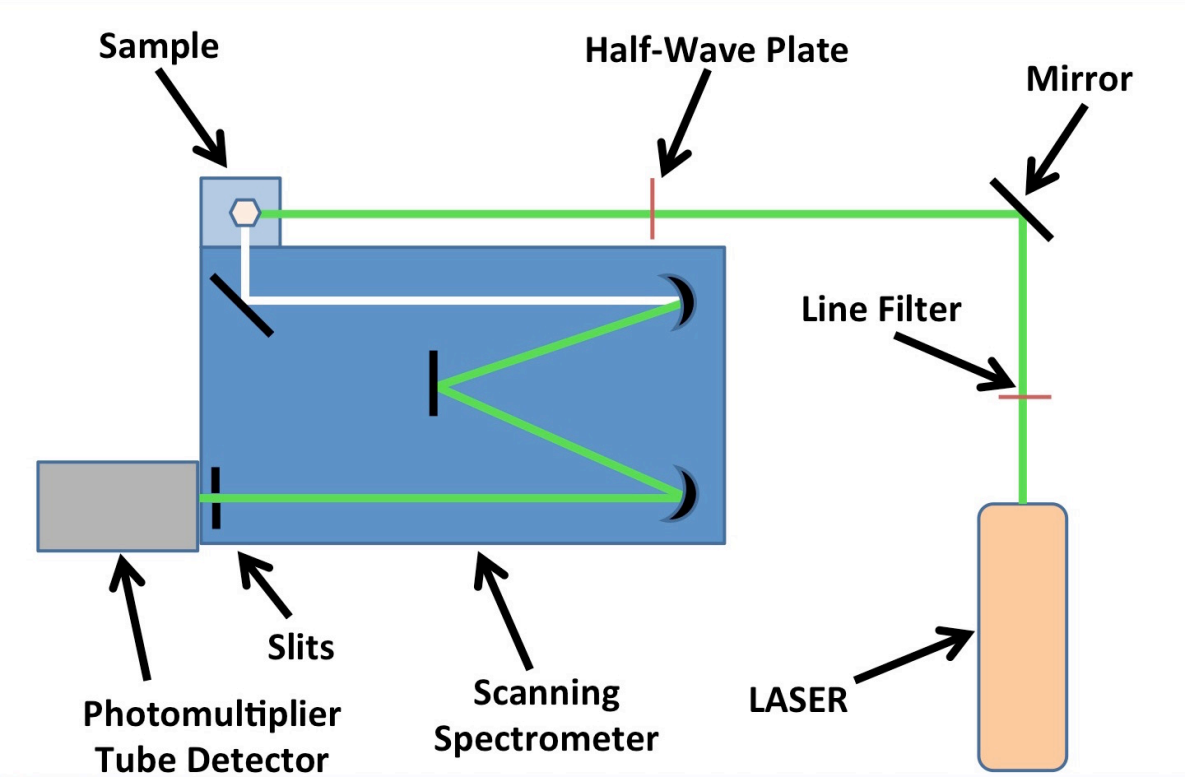

Figure 3.4.1: Schematic of Raman Spectrometer

Laser light with wavelength of 514.5 nm is passed through a line filter, which only allows 514.5 nm radiation to pass through. The mirror reflects this light, focusing it onto the half-wave plate. The half-wave plate rotates the light to the correct polarization. The light is passed through the sample cell, where it excites molecules to a virtual energy state. Scattered photons of light are quickly released from the molecules at a right angle to the incident light. The scattered light enters the scanning spectrometer, and a mirror directs the light onto the first grating. The grating separates the scattered light by wavelength. Then, another mirror reflects the light onto a second grating, where the scattered light is

separated to individual wavelengths. The spectrometer "scans" the scattered light by only allowing single wavelengths of light pass through the slits into the detector. A photomultiplier tube, PMT, is used as a detector because of its extreme sensitivity. The PMT utilizes the photoelectric effect of metals to multiply the signal of a single photon of light. Photons of light enter the PMT, where they collide with the conducting metal. Electrons are emitted from this collision, and they are directed down the multiplier tube. As the electrons travel down the tube, electron collisions cause an increasing number of electrons to be emitted. This cascade of electron emission from a single photon metal collision provides a detectable signal. High sensitivity is necessary for Raman spectroscopy because Raman Stokes scattering only occurs about one in every million photons.

For theoretical calculations, Density Functional Theory, DFT, was used to simulate Raman vibrational frequencies of urea-water and TMAO-urea-water clusters. These calculations were performed using Gaussian 09 software[24] with the B3LYP[25-27] method and a 6-311++g(2df,2pd) basis set.[28-29] Geometrical optimization of structures and the simulation of Raman vibrational frequencies were often performed in one job. To ensure adequate convergence and reliable simulated frequencies, the Gaussian 09 command, "opt=tight", was used to tighten cutoffs on forces and step size used in determining convergence.

CHAPTER 4: RESULTS AND DISCUSSION

In this project, the interaction of TMAO, urea, and water are investigated in two stages. First, in experiment, Raman spectroscopy is used to examine hydrogen bonding in a saturated solution of TMAO and urea in water. The Raman spectra obtained are compared with Raman spectra of a TMAO solution saturated in water and Raman spectra of a urea solution saturated in water. The Raman spectra of the separate urea and TMAO saturated solutions were gathered from previous work done by our lab group.[4] The saturated urea solution had a concentration 11.10 mmol L^{-1}. The saturated TMAO solution had a concentration of 4.44 mmol L^{-1}. Both of these solutions are far more concentrated than concentrations found in nature (See Section 2.3). The TMAO-urea solution had a 1:1 TMAO-urea molar ratio. Next, computational chemistry was used to find low energy structures and theoretical Raman spectra of TMAO, urea and water complexes using Gaussian09 software. These theoretical calculations were used to examine possible molecular interactions occurring in the experimental solution. Furthermore, micro solvation of urea with water was theoretically examined using Gaussian09. Low energy structures of the urea-water complexes and the theoretical Raman spectra obtained were used to determine the possible effects of urea on water hydrogen bonding networks. These results were compared to experimental data of urea and water solutions from previous lab group work.

4.1 Experimental Results

The experimental Raman spectrum of saturated TMAO and urea in water is shown in Figure 4.1.1. The saturated urea spectrum was obtained by Jordan Cauley, who

worked on Raman spectra of experimental urea solvation in the Hammer Lab during the summer of 2014. The saturated TMAO spectrum was obtained from Kristina Cuellar's work on microsolvation of TMAO.[4] The Raman spectrum of saturated urea/TMAO solution was obtained for this thesis.

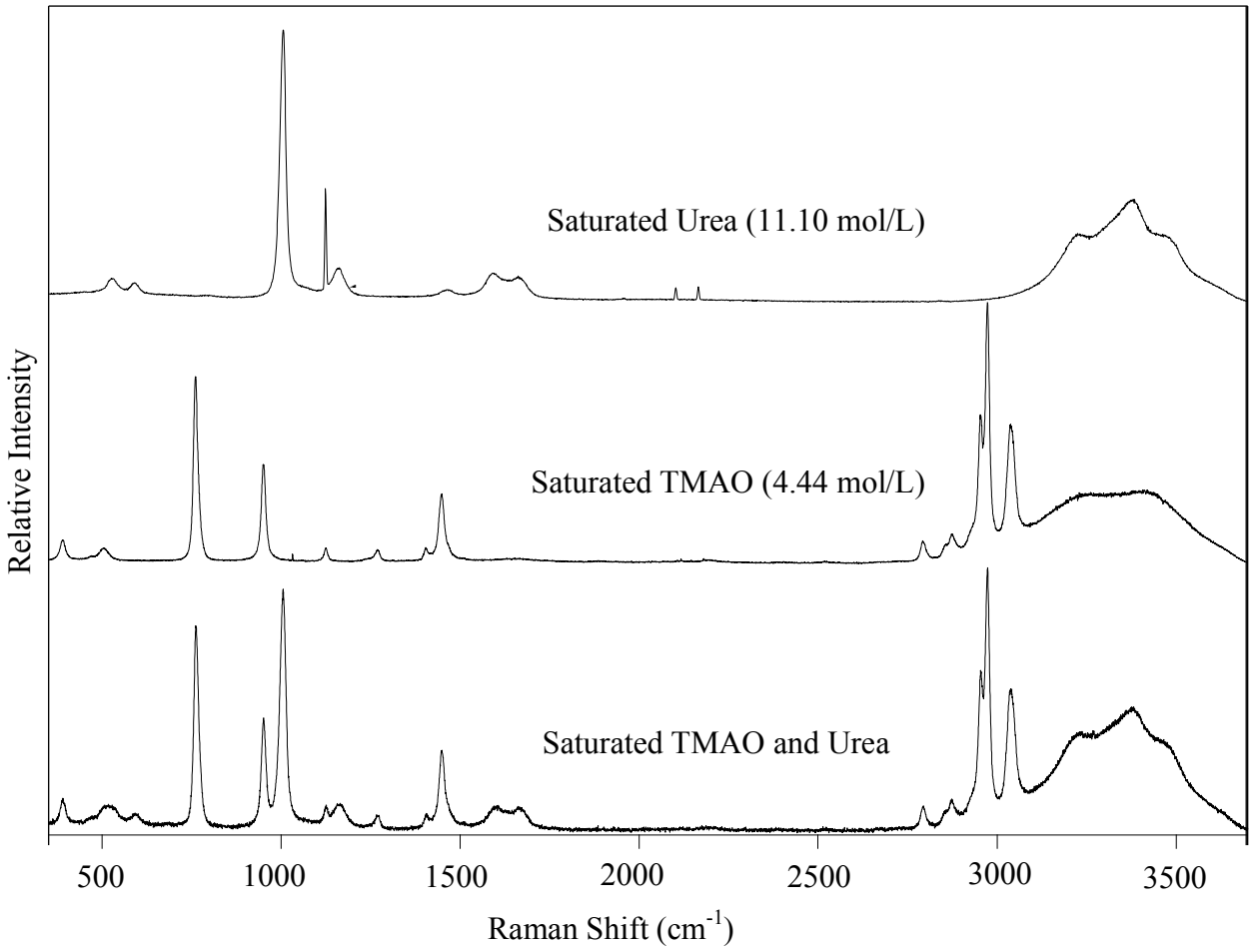

Figure 4.1.1: Raman Spectra of Saturated Urea, Saturated TMAO and Saturated TMAO and Urea

The spectra of all three solutions have common features. The fact that the broad peak around 3400 cm^{-1} is the same intensity for all spectra is a good indication that the solutions are fully saturated. In order to study shifting Raman peaks, which might provide some insight into TMAO-urea interactions in water, a closer look at each peak is needed. Figure 4.1.2 through Figure 4.1.8 show zoomed views of the three experimental spectra.

The motions associated with these peaks are analyzed using the computational results and are discussed in Section 4.3.

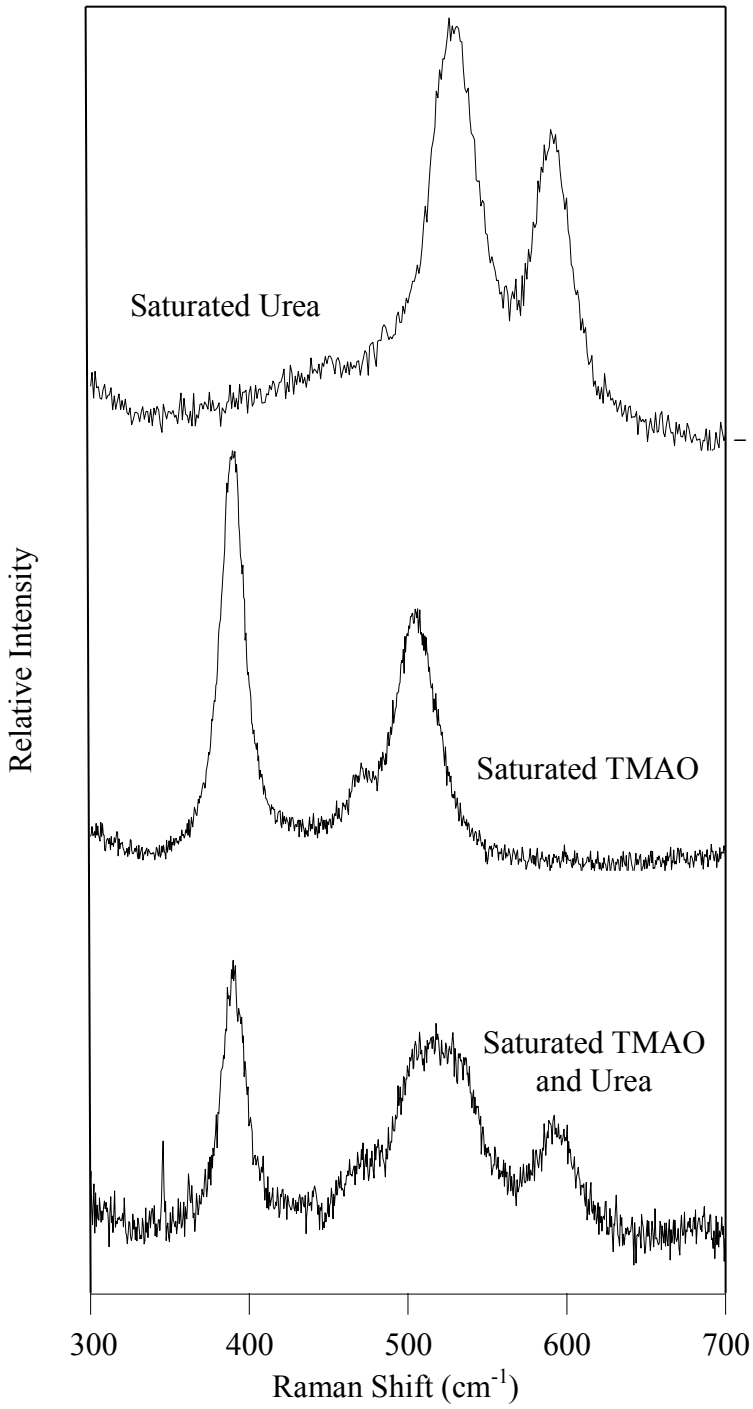

Figure 4.1.2: Experimental Raman Spectra (300-700 cm^{-1})

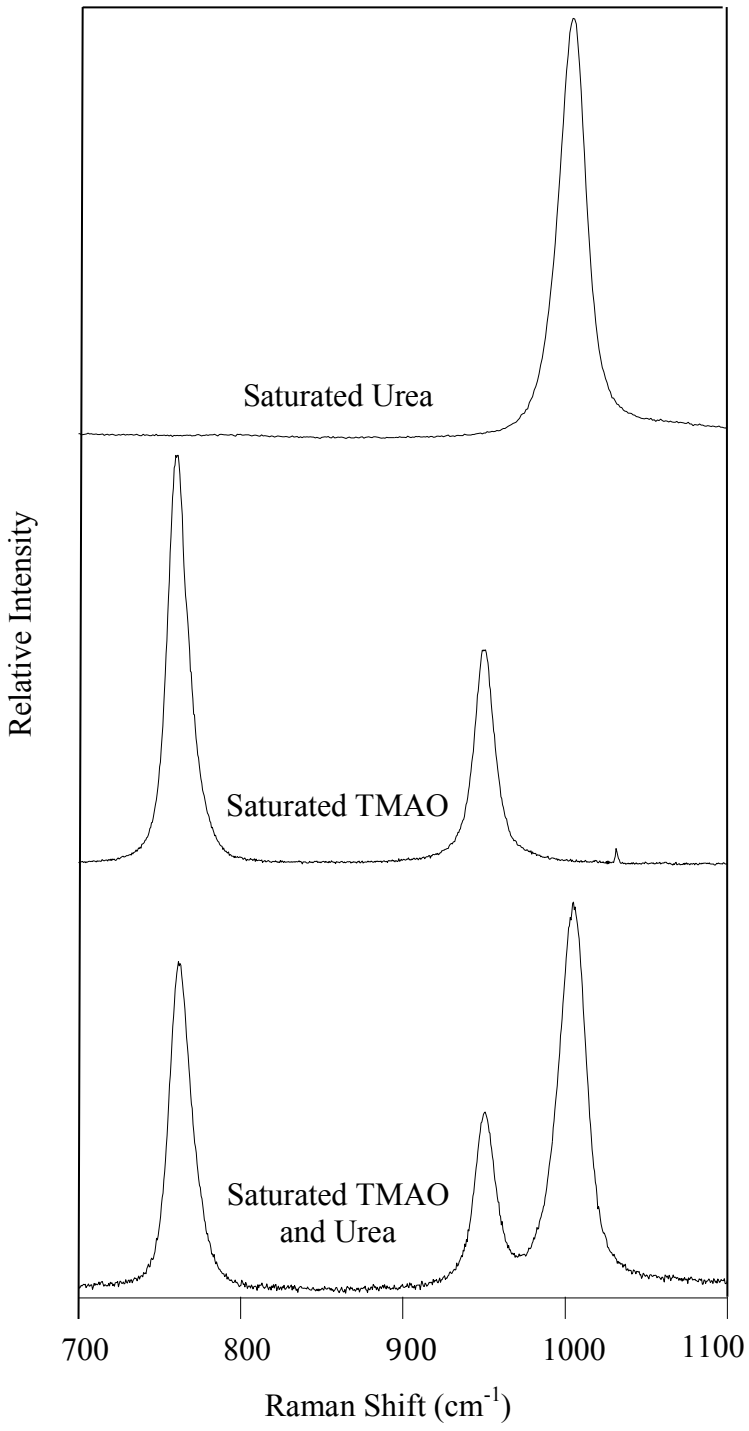

Figure 4.1.3: Experimental Raman Spectra (700-1100 cm^{-1})

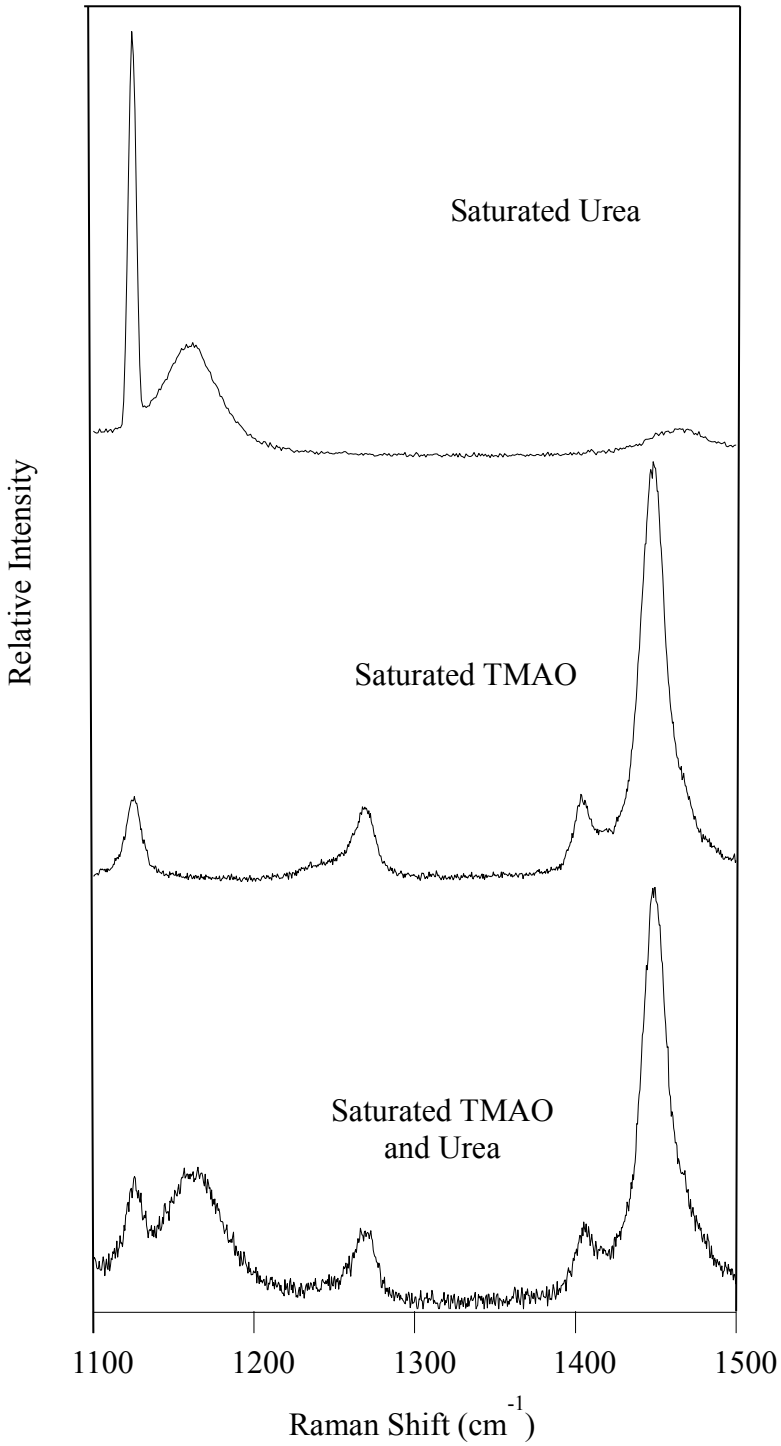

Figure 4.1.4: Experimental Raman Spectra (1100-1500 cm^{-1})

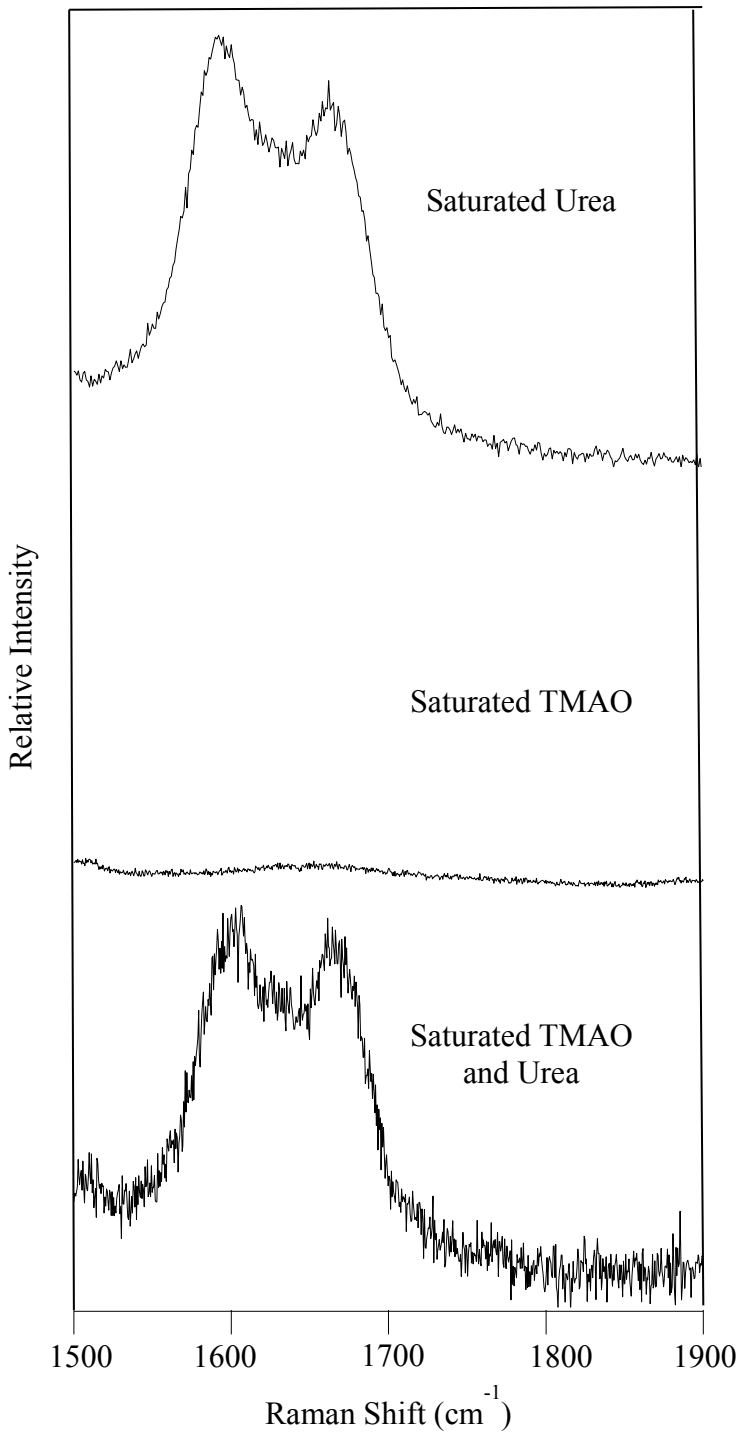

Figure 4.1.5: Experimental Raman Spectra (1500-1900 cm^{-1})

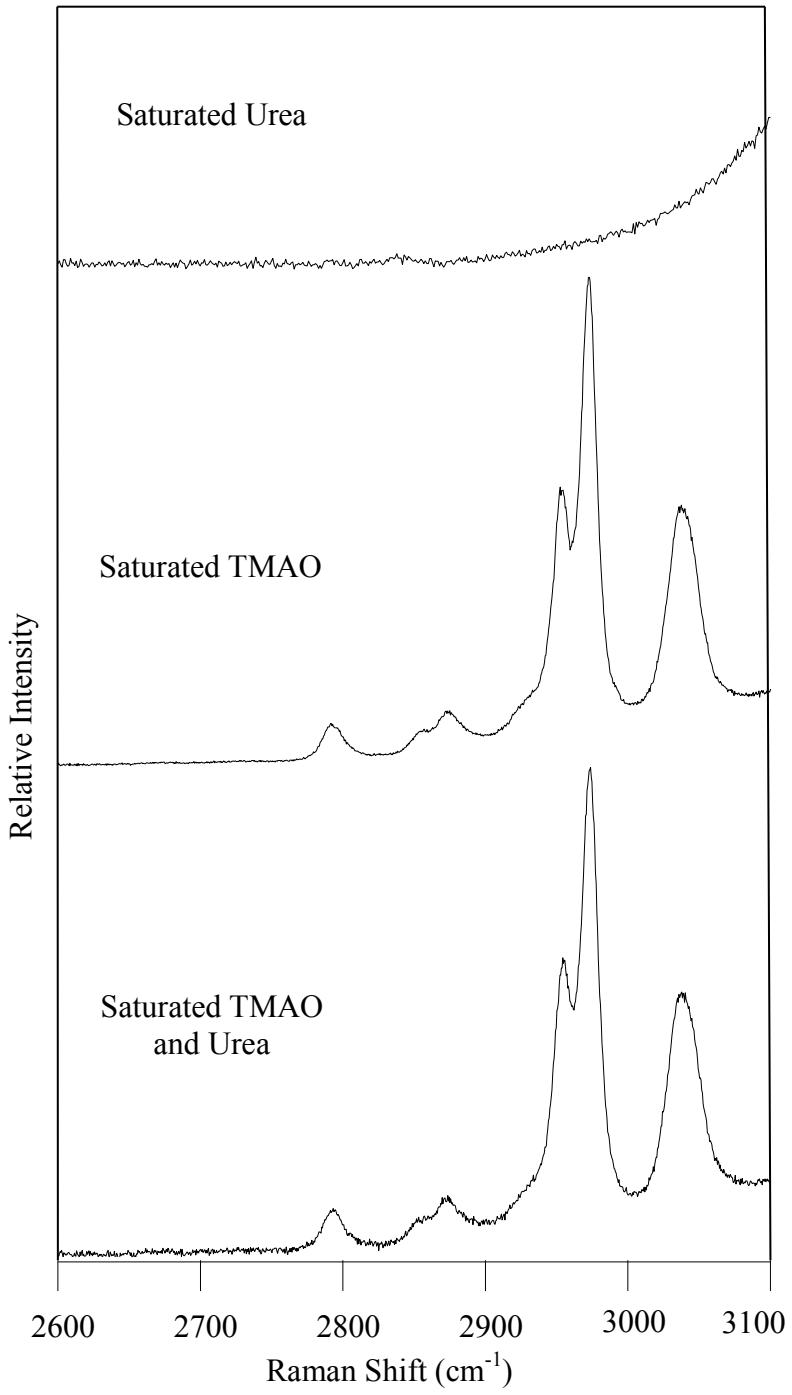

Figure 4.1.6: Experimental Raman Spectra (2600-3100 cm^{-1})

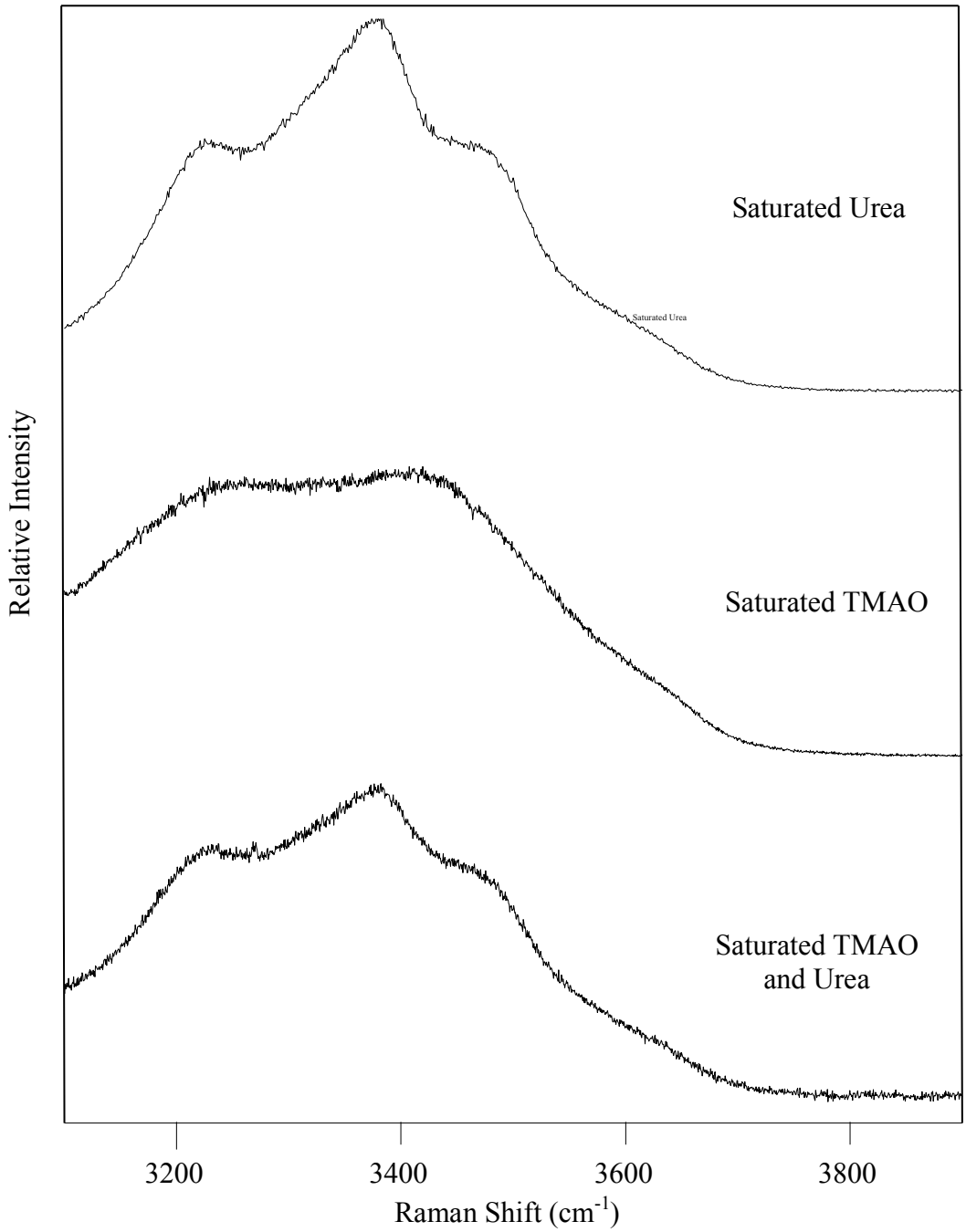

Figure 4.1.7: Experimental Raman Spectra (3100-3900 cm^{-1})

After evaluating each peak along the experimental spectra, there is only one significant shift observed. The only peak that significantly shifted from the individually saturated osmolyte solution to TMAO-urea saturated solution was the vibrational mode at 1592 cm^{-1}. Figure 4.1.8 shows a clear shift when the TMAO-urea spectrum is smoothed out, and Figure 4.1.9 shows saturated urea and saturated TMAO-urea spectra superimposed onto each other.

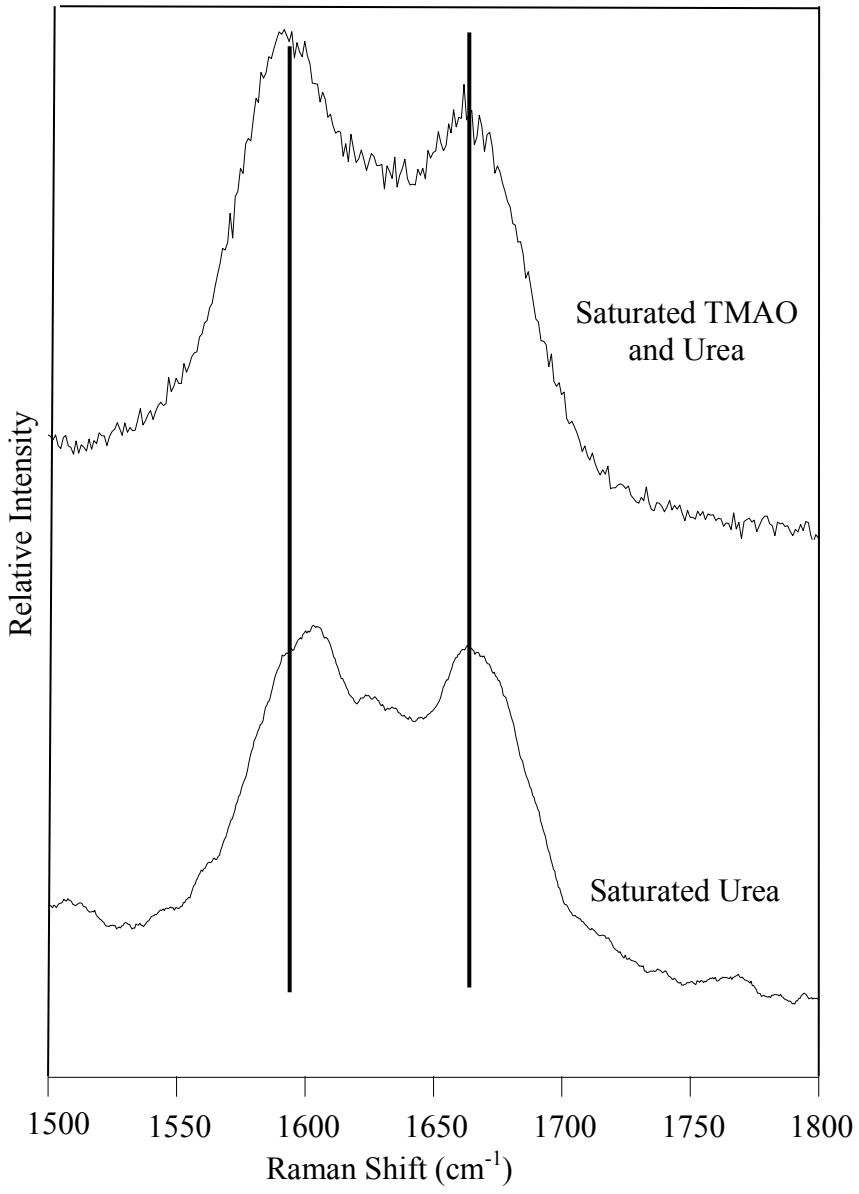

Figure 4.1.8: Urea Raman spectrum and smoothed TMAO-urea Raman spectrum

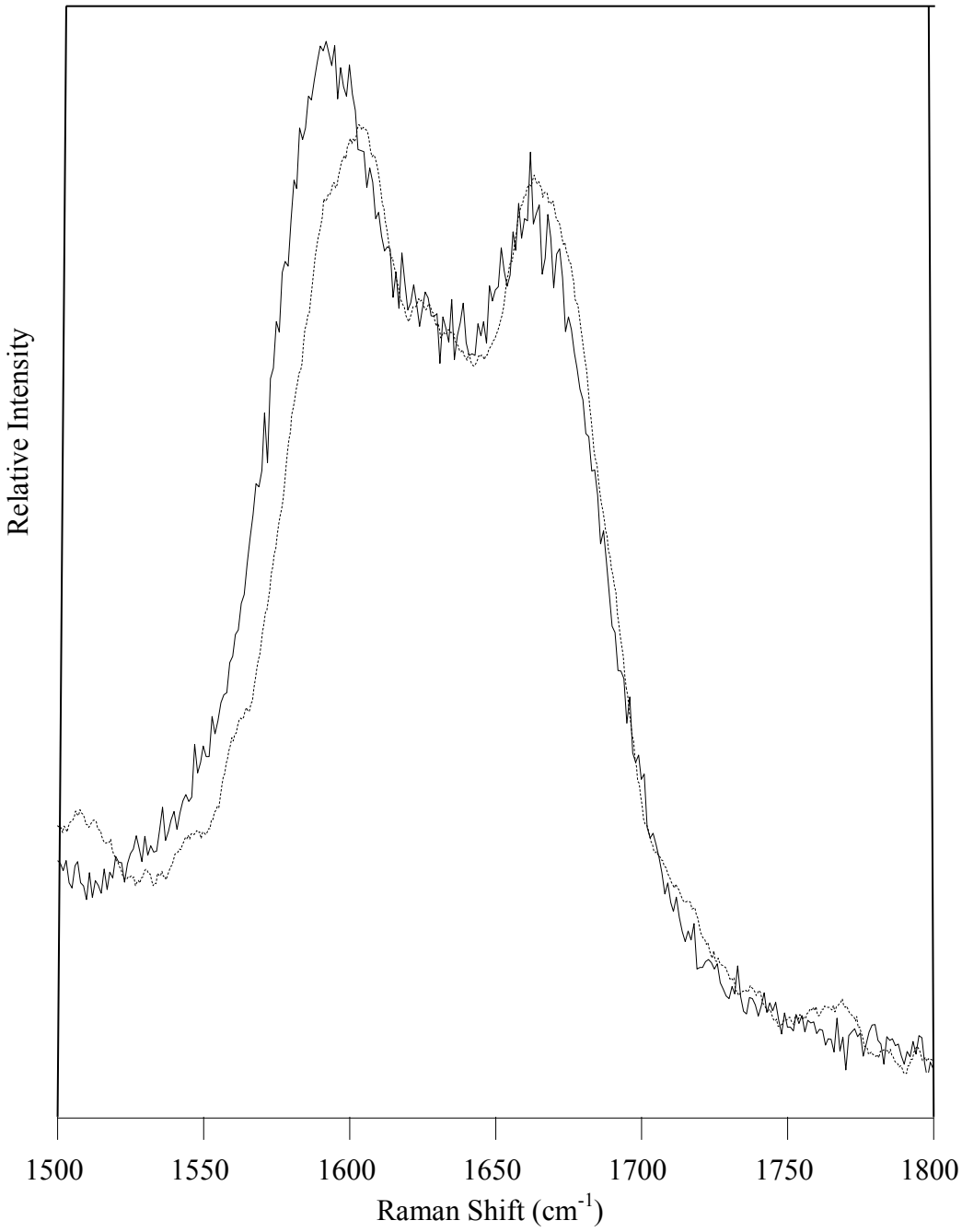

Figure 4.1.9: TMAO-urea spectrum (dotted line) superimposed onto urea spectrum (dark line) (1500-1800 cm^{-1})

Interestingly, the other vibrational mode in the spectra above, at 1662 cm^{-1}, does not significantly shift (-1cm^{-1}), while mode at 1592 cm^{-1} blue shifts by 11 cm^{-1}. Furthermore, the shifted mode seems to lose intensity in the solution of TMAO, urea and

water. The comparison of modes in the three experimental spectra are summarized in Table 4.1.1 and 4.1.2.

Peak in Saturated TMAO solution (cm^{-1})	Peak in Saturated TMAO-Urea Solution (cm^{-1})	Raman Peak Shift (cm^{-1})
3037	3038	1
2972	2974	2
2952	2954	2
2873	2874	1
2791	2793	2
1448	1450	2
1403	1405	2
1267	1271	4
1125	1126	1
950	951	1
761	762	1
389	390	1

Table 4.1.1: Summary of Experimental TMAO Peaks

TMAO vibrational modes in Raman spectra see almost no shifting when urea is added to solution. In fact, the only TMAO vibrational mode that shifts more than 2 cm^{-1} is that starting at 1267 cm^{-1} (4 cm^{-1}). In Figure 4.1.11, urea vibrational modes also have very small peak shifts when TMAO is added to solution. However, the mode initially at 1592 shifts 11 cm^{-1} when TMAO is added to solution.

Peak in Saturated Urea solution (cm^{-1})	Peak in Saturated TMAO-Urea Solution (cm^{-1})	Raman Peak Shift (cm^{-1})
3382	3382	0
1662	1661	-1
1592	1603	11
1162	1162	0
1005	1005	0
590	592	2

Table 4.1.2: Summary of Experimental Urea Peaks

All but one of the urea vibrational modes shifts by 2 cm^{-1} or less. In order to elucidate what vibration is coupled with this shifted vibrational mode, theoretical data must be evaluated and compared to experimental data. Possible simulated structures of the solutions are used as a microscopic view of the interactions between TMAO, urea and water.

4.2 Theoretical Results

The goal of the theoretical work in this project was to elucidate the origin of the experimental spectra shift starting at 1592 cm^{-1}. First, the optimized three water-TMAO (C_{3v} symmetry) structure from Kristina Cuellar's work is reproduced in Figure 4.2.1[10]. Figures 4.2.2 through 4.2.4 show optimized urea (C_2 symmetry) water structures, obtained using Gaussian09.

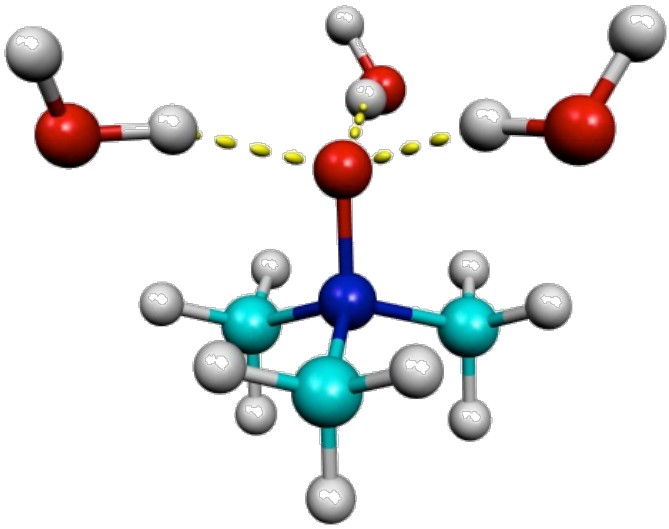

Figure 4.2.1: Optimized Structure of TMAO with Three Waters[4]

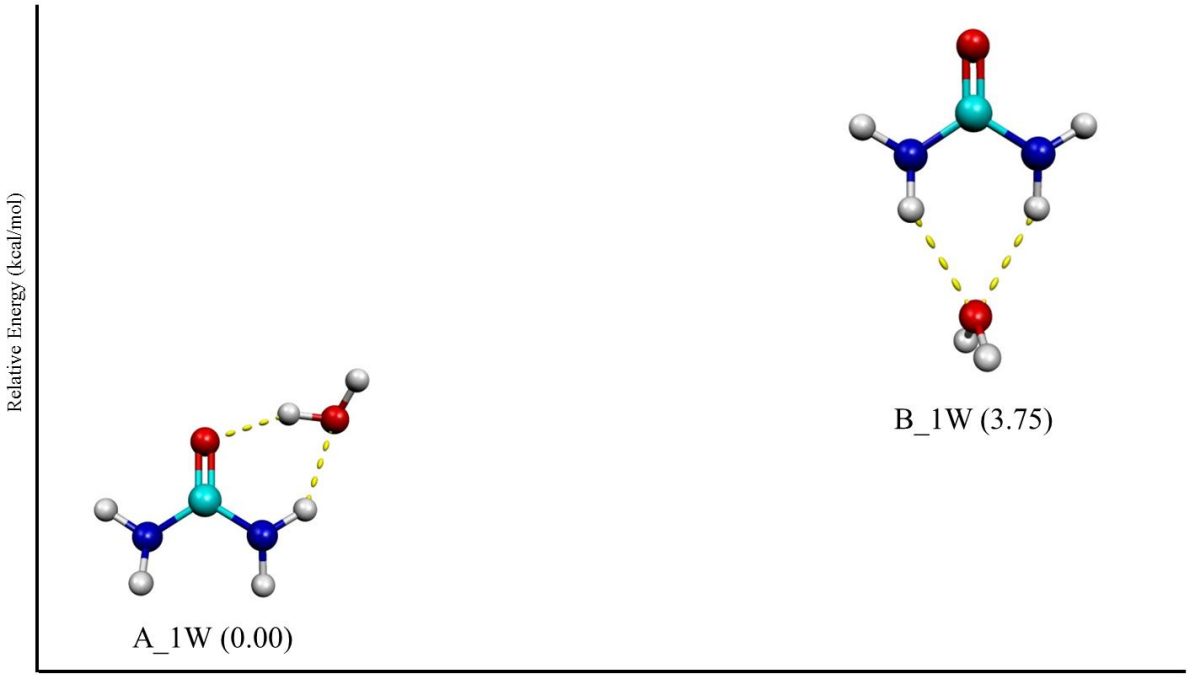

Figure 4.2.2: Optimized Structures of Urea with One Water. Relative Energies are in kcal/mol.

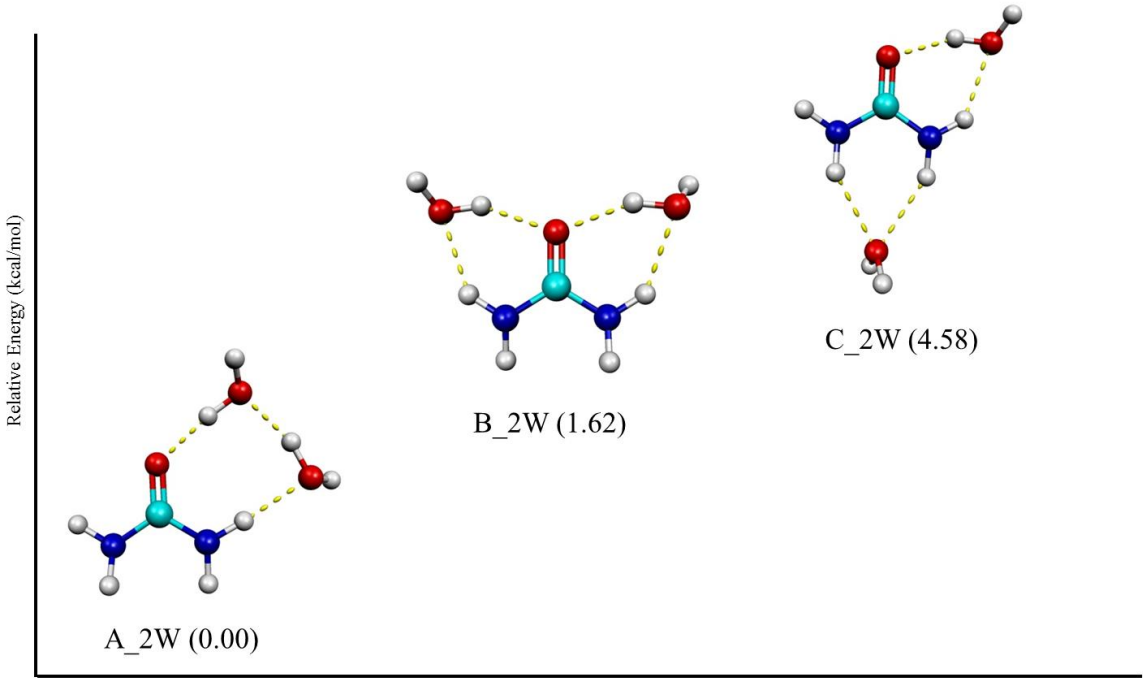

Figure 4.2.3: Optimized Structures of Urea with Two Waters. Relative Energies are in kcal/mol.

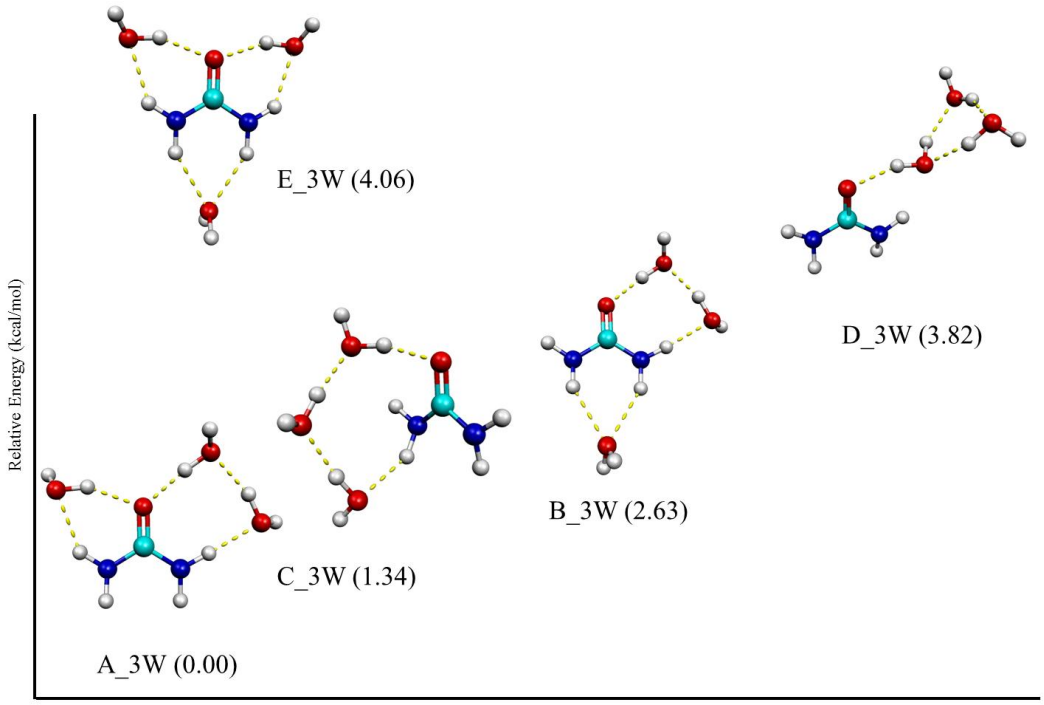

Figure 4.2.4: Optimized Structures of Urea with Three Waters. Relative Energies are in kcal/mol.

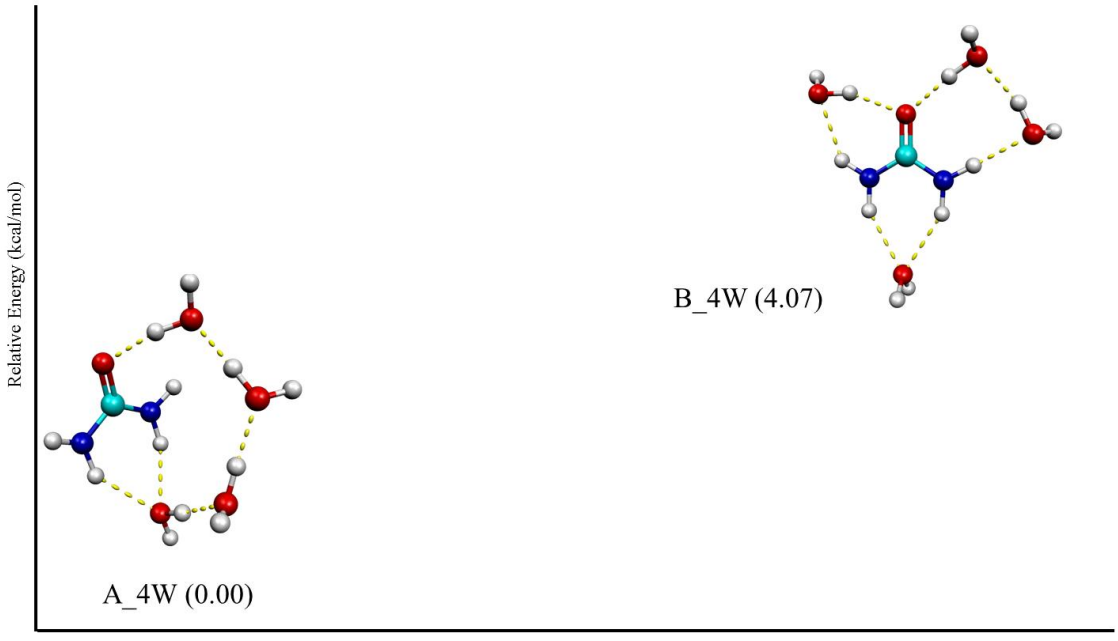

Figure 4.2.5: Optimized Structures of Urea with Four Waters. Relative Energies are in kcal/mol.

Although a five water-urea structure has been reported in literature[30], it is not clear whether urea structures with different numbers of waters have been extensively studied. Many urea-water optimized structures were found in this experiment, although there are likely many more that were not investigated. The lowest energy urea-water structures show possible interaction sites for water and TMAO. Also, the urea-water structures (especially three water structures) are used as a starting template for TMAO addition. Table 4.2.1 shows the binding energies for each urea-water complex along with its relative energy in kcal mol^{-1}.

Urea-Water *Figure 4.2.2*	Binding Energy (kcal mol^{-1})	Relative Energy (kcal mol^{-1})
A_1W	-9.03	0.00
B_1W	-5.28	3.75
Urea-2Water *Figure 4.2.3*		
A_2W	-19.38	0.00
B_2W	-17.76	1.62
C_2W	-14.83	4.58
Urea-3Water *Figure 4.2.4*		
A_3W	-27.88	0.00
C_3W	-26.55	1.34
B_3W	-25.25	2.63
D_3W	-24.06	3.82
E_3W	-23.82	4.06
Urea-4Water *Figure 4.2.5*		
A_4W	-38.15	0.00
B_4W	-34.08	4.07

Table 4.2.1: Binding Energies for All Urea-Water Structures (kcal mol^{-1})

Furthermore, optimized structures of TMAO-urea dimers with increasing water molecules were found using Gaussian09. The optimized dimer structures are shown in Figure 4.2.6 through Figure 4.2.9.

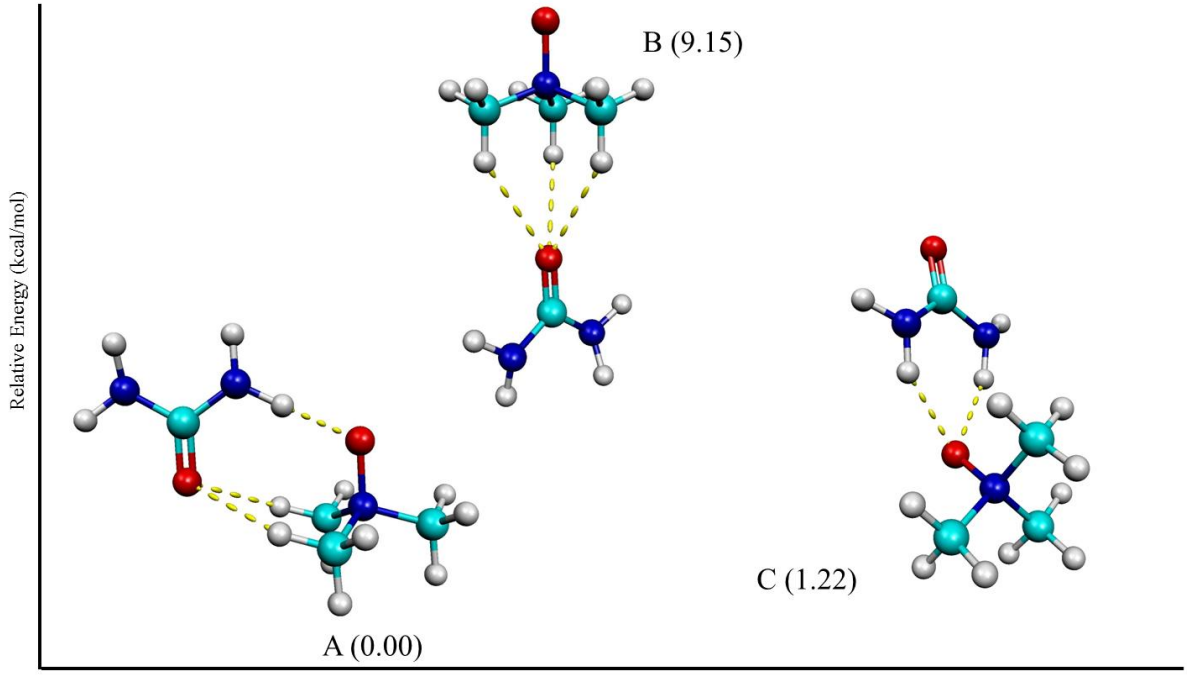

Figure 4.2.6: Optimized Dimer Structures. Relative Energies are in kcal/mol.

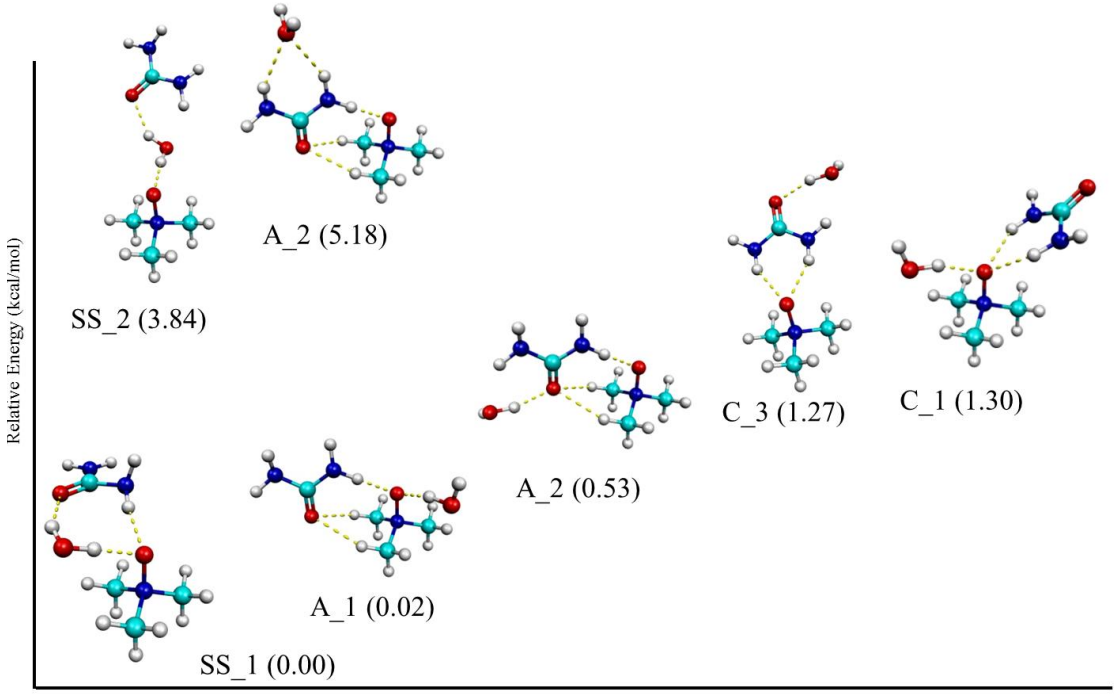

Figure 4.2.7: Optimized Dimer Structures with One Water. Relative Energies are in kcal/mol.

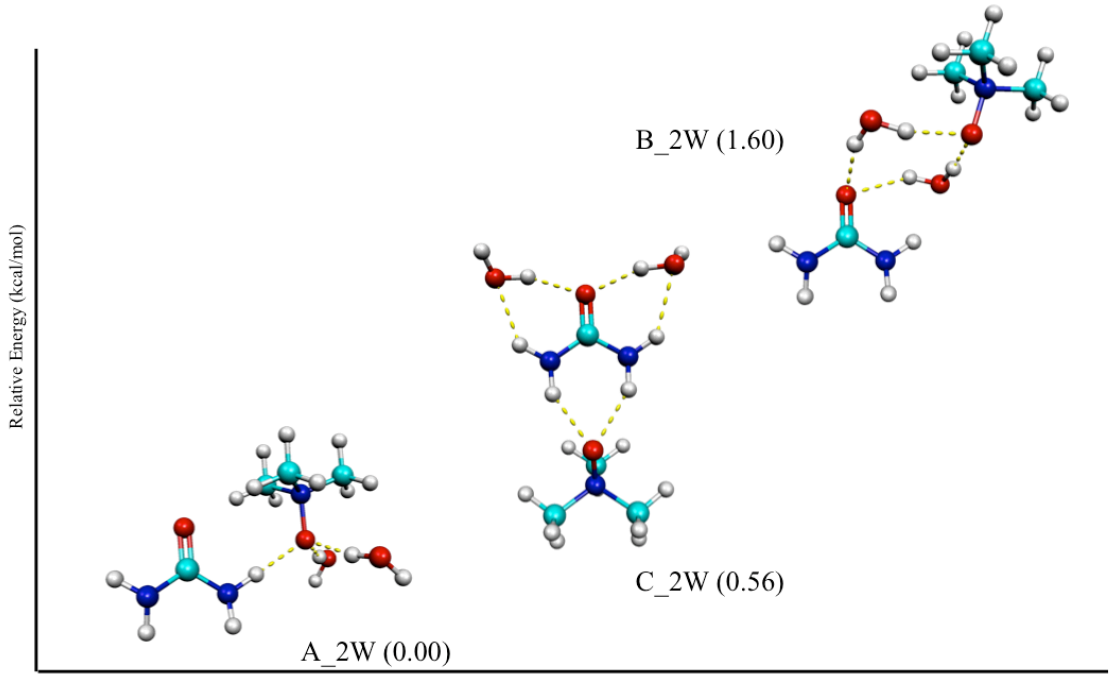

Figure 4.2.8: Optimized Dimer Structures with Two Waters. Relative Energies are in kcal/mol.

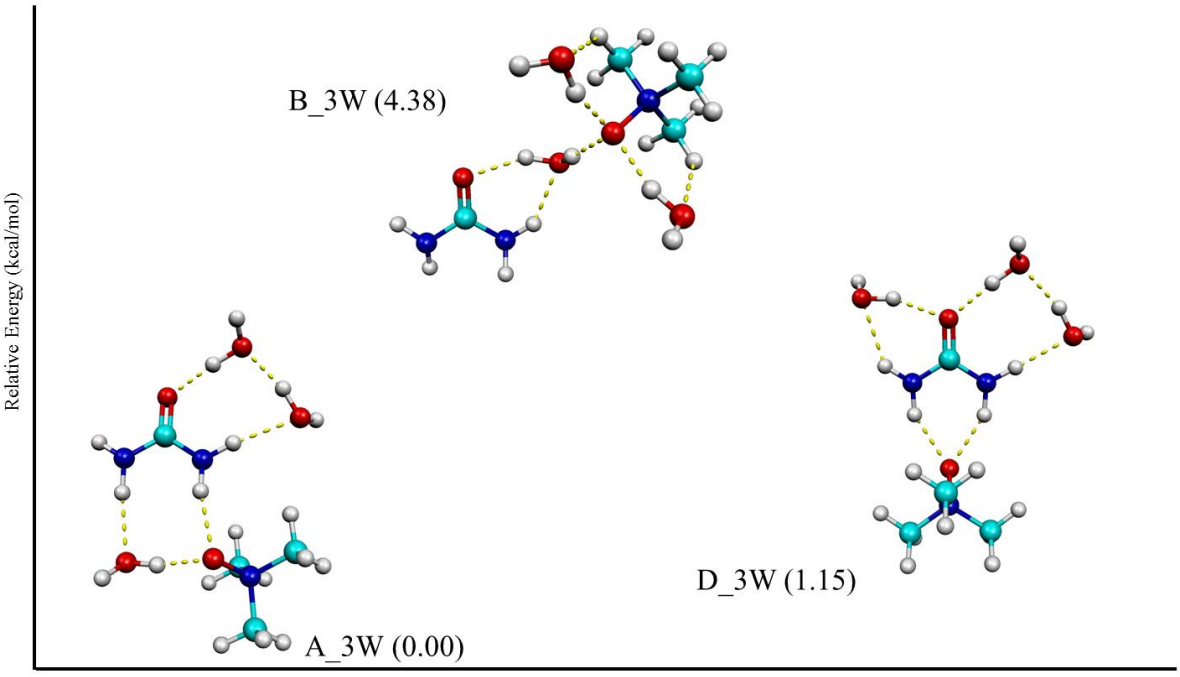

Figure 4.2.9: Optimized Dimer Structures with Three Waters. Relative Energies are in kcal/mol.

These structures represent only a few optimized structures for each level of hydration. The binding energies for the TMAO-urea-water complexes can be found in Table 4.2.2 along with relative energies in kcal mol^{-1}. The optimized structures were used to find possible structures that are found in nature; however, the relevant data for experimental comparison is how the 1592 cm^{-1} mode shifts in theory.

TMAO-Urea *Figure 4.2.6*	Binding Energy (kcal mol^{-1})	Relative Energy (kcal mol^{-1})
A	-13.05	0.00
C	-11.92	1.22
TMAO-Urea-1Water *Figure 4.2.7*		
SS_1	-22.88	0.00
A_1	-22.87	0.02
A_3	-22.22	0.53
C_3	-21.56	1.27
C_1	-21.68	1.30
SS_2	-18.99	3.84
A_2	-17.57	5.18
TMAO-Urea-2Water *Figure 4.2.8*		
A_2W	-31.51	0.00
C_2W	-30.96	0.56
B_2W	-29.29	1.60
TMAO-Urea-3Water *Figure 4.2.9*		
A_3W	-42.34	0.00
D_3W	-41.23	1.15
B_3W	-38.00	4.38

Table 4.2.2: Binding Energies for All TMAO-Urea-Water Structures (kcal mol^{-1})

Raman frequencies for each of the lower energy structures were calculated using Gaussian09. The dimer and urea structures with similar water placement are compared to each other. After observing theoretical vibrational modes in GaussView, it is clear that the peaks around 1600 cm^{-1} belong to HNH bends in urea and HOH bends in water. The mode that shifts is most likely the symmetrical HNH bend, usually the first distinguishable peak in the area around 1600 cm^{-1}.

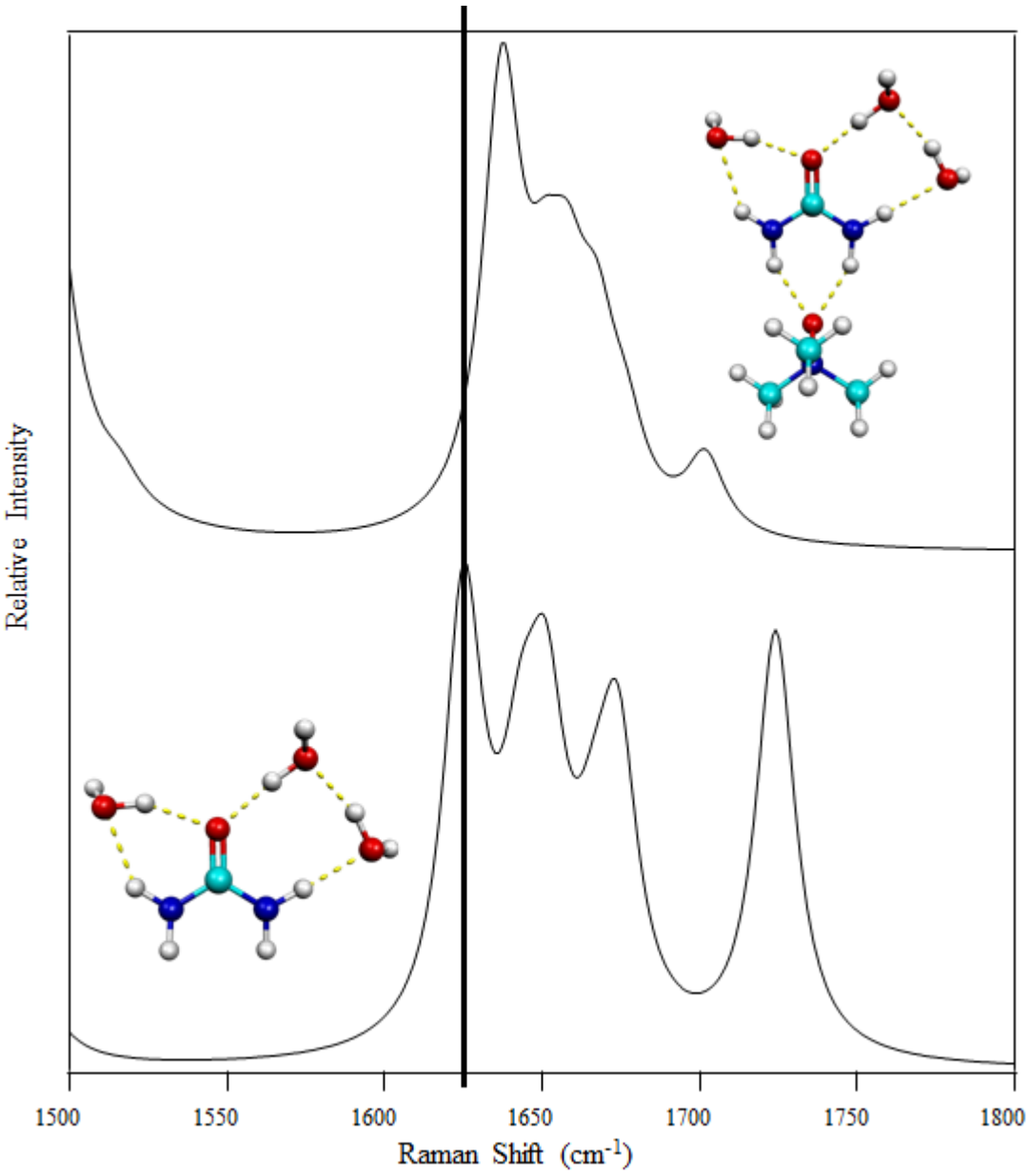

Figure 4.2.10: Theoretical Raman Spectral Shift of HNH symmetric bend

Figure 4.2.10 shows a Raman spectrum of the lowest energy urea-3water structure (A_3W) compared to a Raman spectrum of the second lowest energy dimer-3water structure (D_3W). The two are compared because waters in both structures hydrogen bond at the top of the urea molecule. The TMAO can be thought of as "added" to the

bottom of the urea structure. The theoretical HNH symmetrical bend of urea starting at 1625 cm^{-1} is blue shifted by 12 cm^{-1}.

Although simulating the TMAO urea interaction as TMAO being "added" to the urea-water clusters is useful, having a TMAO molecule replace a water molecule around the urea is a more accurate simulation of experimental TMAO-urea interaction.

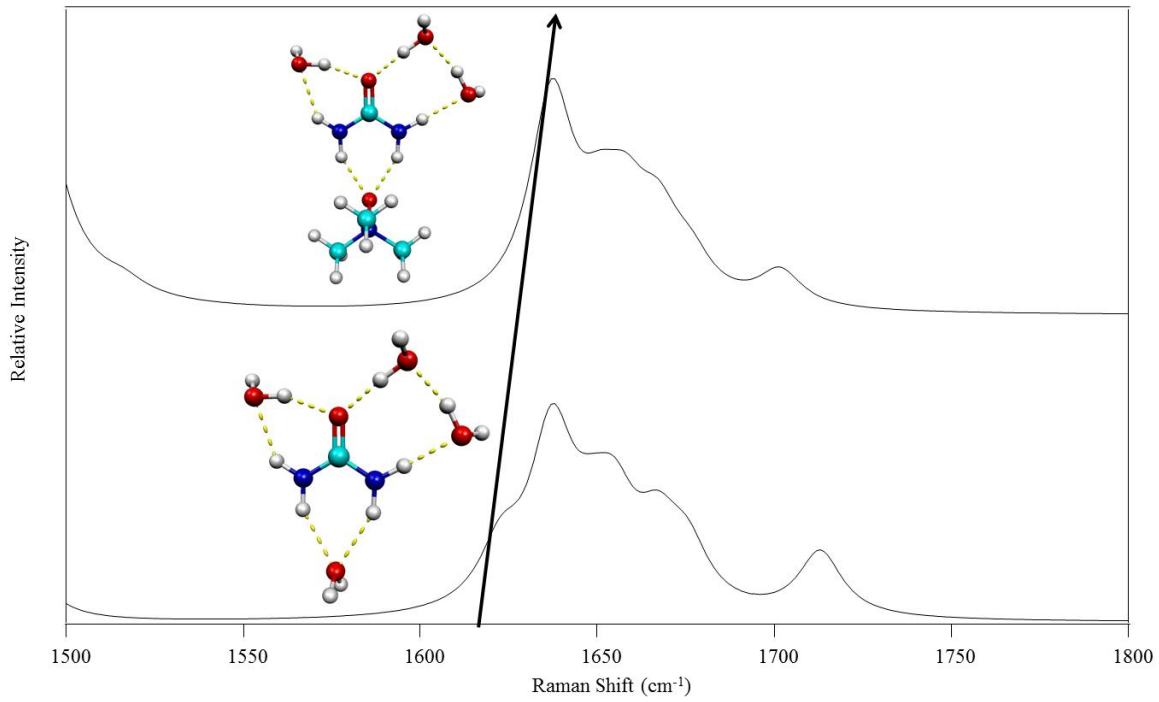

Figure 4.2.11: Theoretical Raman Spectral Shift of TMAO replacing water

Figure 4.2.11 shows a theoretical Raman shift between the second lowest energy four water-urea structure (B_3W from Figure 4.2.5) and the second lowest energy three water-TMAO-urea structure (B_3W from Figure 4.2.9). This Raman spectral shift is a clear blue shift that resembles the experimental shift.

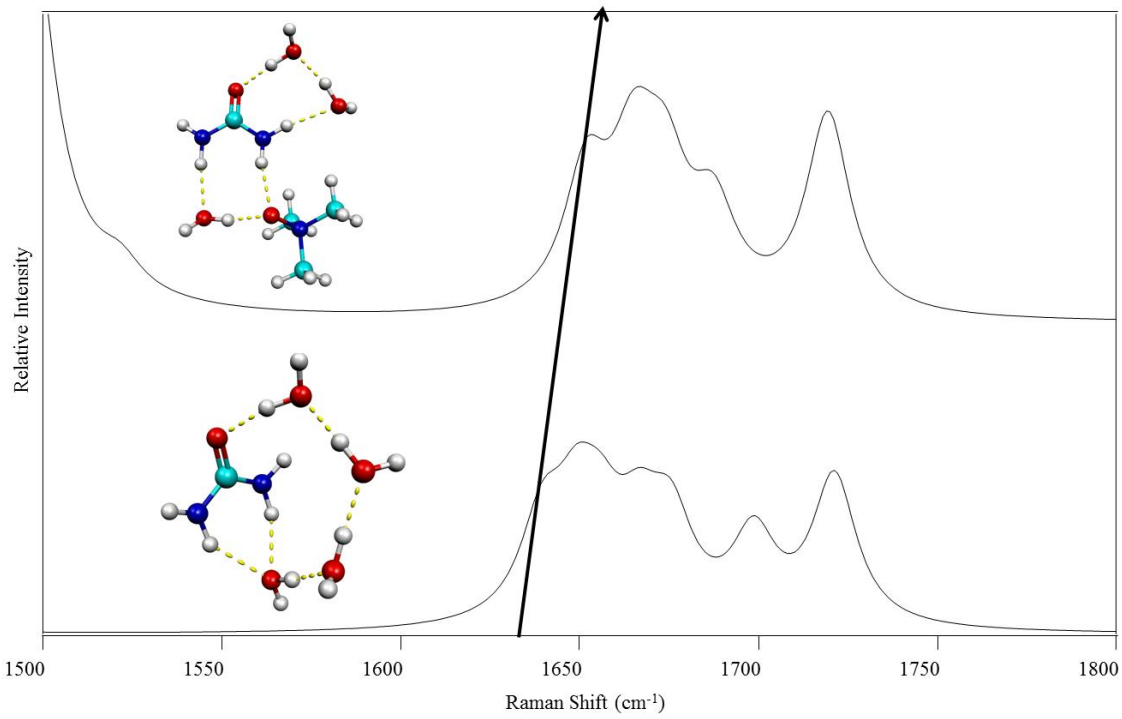

Figure 4.2.12: Theoretical Raman Spectral Shift of TMAO replacing water

Finally, Figure 4.2.12 shows another theoretical Raman shift when TMAO replaces water around the urea. In this figure, the lowest energy four water-urea structure (A_4W from Figure 4.2.5) is compared to the lowest energy three water-TMAO-urea structure (A_3W from Figure 4.2.9). Although there is a clear shift of urea bending modes in this theoretical comparison, it is the asymmetric bending mode that shifts instead of the symmetric bending mode.

4.3 Comparison of Experimental and Theoretical Data

In order to understand the experimental blue shift of the 1592 cm^{-1} peak, theoretical Raman spectra were used to assign the experimental Raman spectra. In the case of this experiment, the optimized structures can aid in characterizing the vibrational mode that is found blue shifted in experiment.

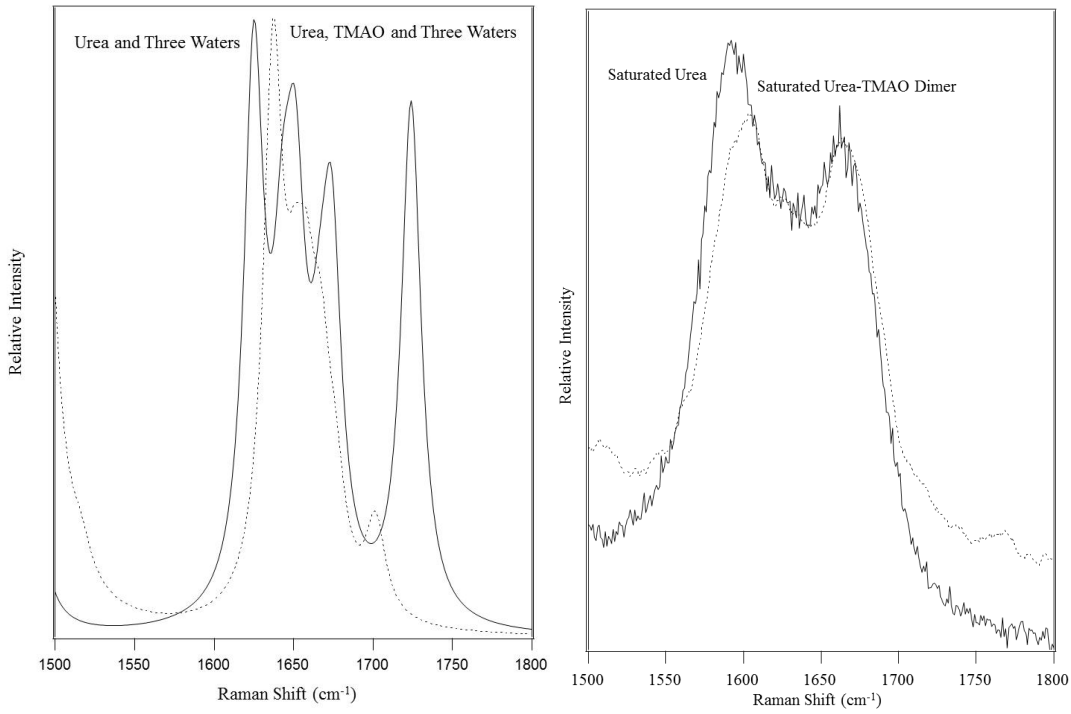

Figure 4.3.1: Comparison of Theoretical (structure A_3W urea and D_3W dimer) (Left) and Experimental (Right) Blue Shifting of symmetric HNH urea bend.

It is clear that both theory and experiment show a blue shift of a urea vibrational mode when TMAO is added to solution (see Figure 4.3.1). Theoretical Raman spectra show many more significant shifts, where experimental spectra show only one. For example, a comparison between the HNH symmetric bend of urea-three water structure (B_3W) and dimer-three water structure (A_3W) shows a 15 cm^{-1} red shift, an energy shift in the opposite direction observed in experiment. This discrepancy between experiment and theory suggests that those two theoretical structures are not found in nature. Another comparison of 3 water structure spectra (urea A_3W vs. TMAO-urea D_3W) (Table 4.2.1) shows a 15 cm^{-1} blue shift of the HNH symmetric bend, which is almost identical to the experimental blue shift. A comparison of these two structures' Raman spectra is shown in Figure 4.3.1 (Left). Finally, experimental and theoretical Raman spectra can be compared to determine the likely structures present in solution. If these theoretical

spectra match experimental spectra well, the structures found in the experimental solutions will likely mirror these structural motifs.

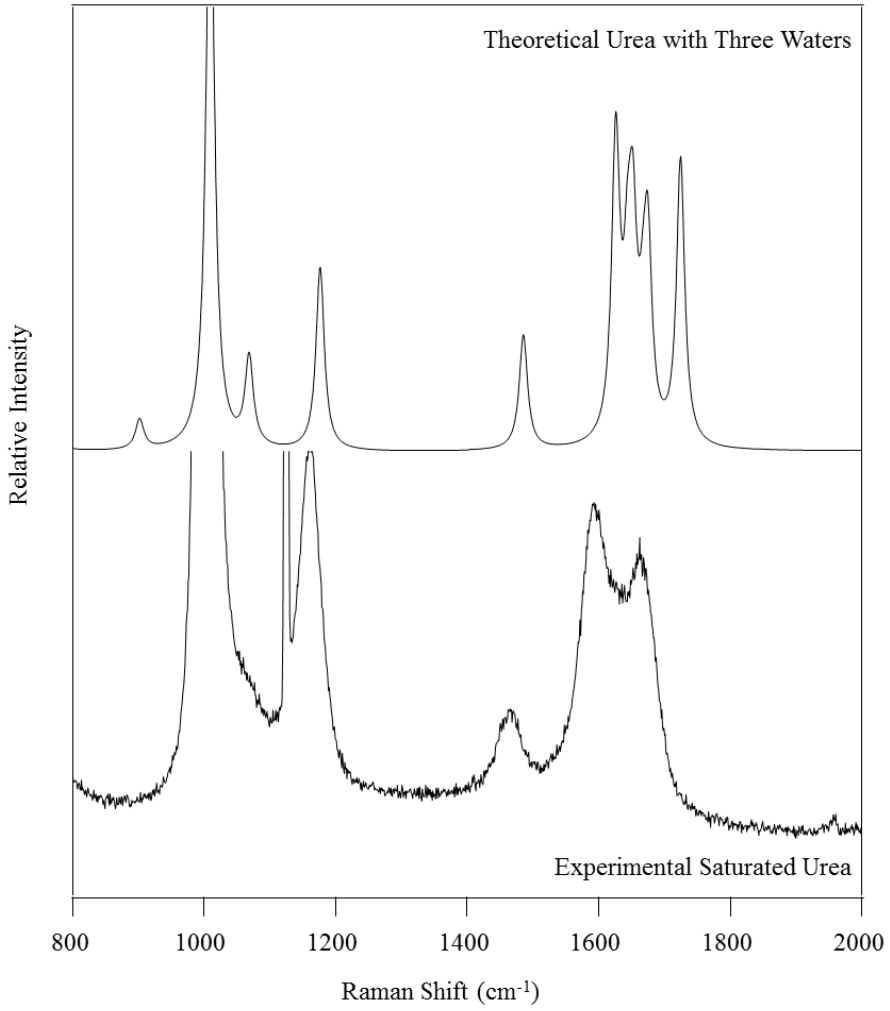

Figure 4.3.2: Experimental vs. Theoretical Urea-Water Raman Spectra.

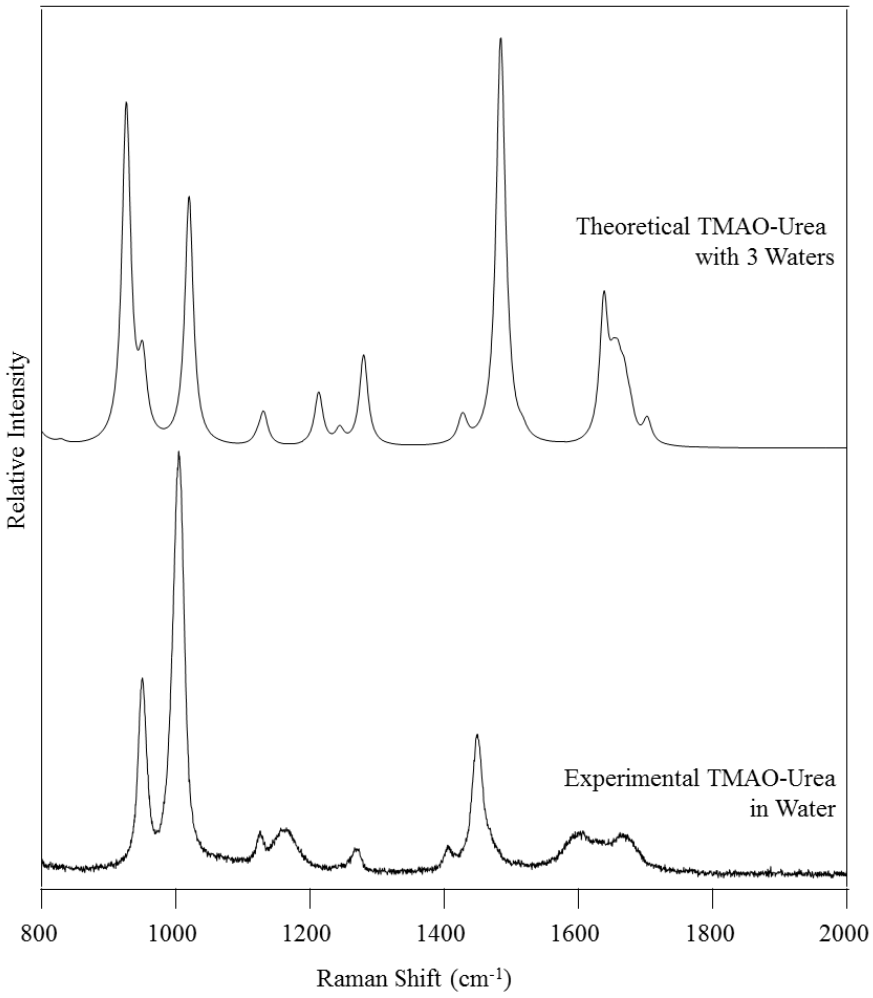

Figure 4.3.3: Experimental vs. Theoretical TMAO-Urea-Water Raman Spectra.

Figures 4.3.2 and 4.3.1 compare theoretical and experimental Raman spectra for urea-water solutions and dimer-water solutions from 800 cm^{-1} to 2000 cm^{-1}. The theoretical spectra seem to match the experimental spectra well. The structure used for the theoretical spectrum in Figure 4.3.2 is urea-3 water A_3W (Figure 4.2.4), and the structure used for the theoretical spectrum in Figure 4.3.3 is TMAO-urea-3 water D_3W (Figure 4.2.9).

4.4 Discussion of Results

The overall goal of this experiment is to investigate the mechanism through which TMAO counteracts urea's ability to denature proteins. It has been cited in literature that TMAO will protect protein stability in the presence of urea when TMAO is present in the cell with at least half the concentration of urea (2:1 urea:TMAO concentration ratio).[17] The hypothesis that TMAO outcompetes urea for protein interaction has been investigated, but the hypothesis that TMAO might directly interact with urea has not been studied extensively[17]. This experiment uses experimental and theoretical Raman frequencies to study the possible interactions between TMAO, urea and water. The experimental data shows only one significant Raman shift: a blue shift of HNH symmetric urea bending mode (Figure 4.1.8). The theoretical Raman spectra aided in the identification of the blue shift as a HNH urea bend. Most theoretical spectra show a similar blue shift in HNH symmetric urea bending mode (Table 4.2.1), but there are many other shifts that are not observed in experimental data. The most hydrated theoretical structure is likely to be the most accurate simulation of saturated experimental solutions, but a complete saturation theoretical structure is impossible to calculate. Instead, it is important to analyze urea structures that have the most affected interaction spots filled with either water or TMAO. The solvation of urea shown in section 4.2.1 provides insight into urea's favorable interaction sites. Water molecules aggregate to either side of the carbonyl oxygen on urea and in between the two amine groups of urea. Every low energy structure found contains waters at one of these sites, even though many calculations at other binding sites were attempted. It is interesting that the optimized three-water urea structure with a water ring (Figure 4.2.4 D_3W) is actually the highest

energy structure found with three waters. TMAO-water structures, where waters interact with each other instead of around TMAO, have been shown to have the lowest energy of any TMAO-water structure in our group's previous work[4]. Instead, the lower energy urea three-water structures prefer to split the waters (Figure 4.2.4 A_3W and B_3W). This data seems to support the literature arguments that urea destabilizes hydrogen bonding networks, freeing water molecules to attack protein structures[3]. The most hydrated dimer structures (3 water) show that structures with the TMAO interacting with amine groups of the urea are lowest in energy. Interestingly, low energy structures of this hydrated dimer, show that water molecules preferentially interact above urea, with its carbonyl group (Figure 4.2.9 A_3W and D_3W). In addition, the blue shift of the HNH symmetric bend, found in experiment, is only seen in theory when the TMAO molecule is found below the urea molecule with its oxygen group acceptor and the amine hydrogen atoms acting as hydrogen bond donors. The fact that these structures (Figure 4.2.9 A_3W and D_3W) are the two lowest in energy and that the blue shift of the urea HNH bend is only found in structures with TMAO's oxygen hydrogen-bonding with amine hydrogen atoms supports the hypothesis that TMAO directly interacts with urea to counter urea's denaturation. The other possible cause of the urea bending blue shift seen in experiment is water molecule interaction with urea. However, theoretical data, shown in Figure 4.4.1, refutes this possibility.

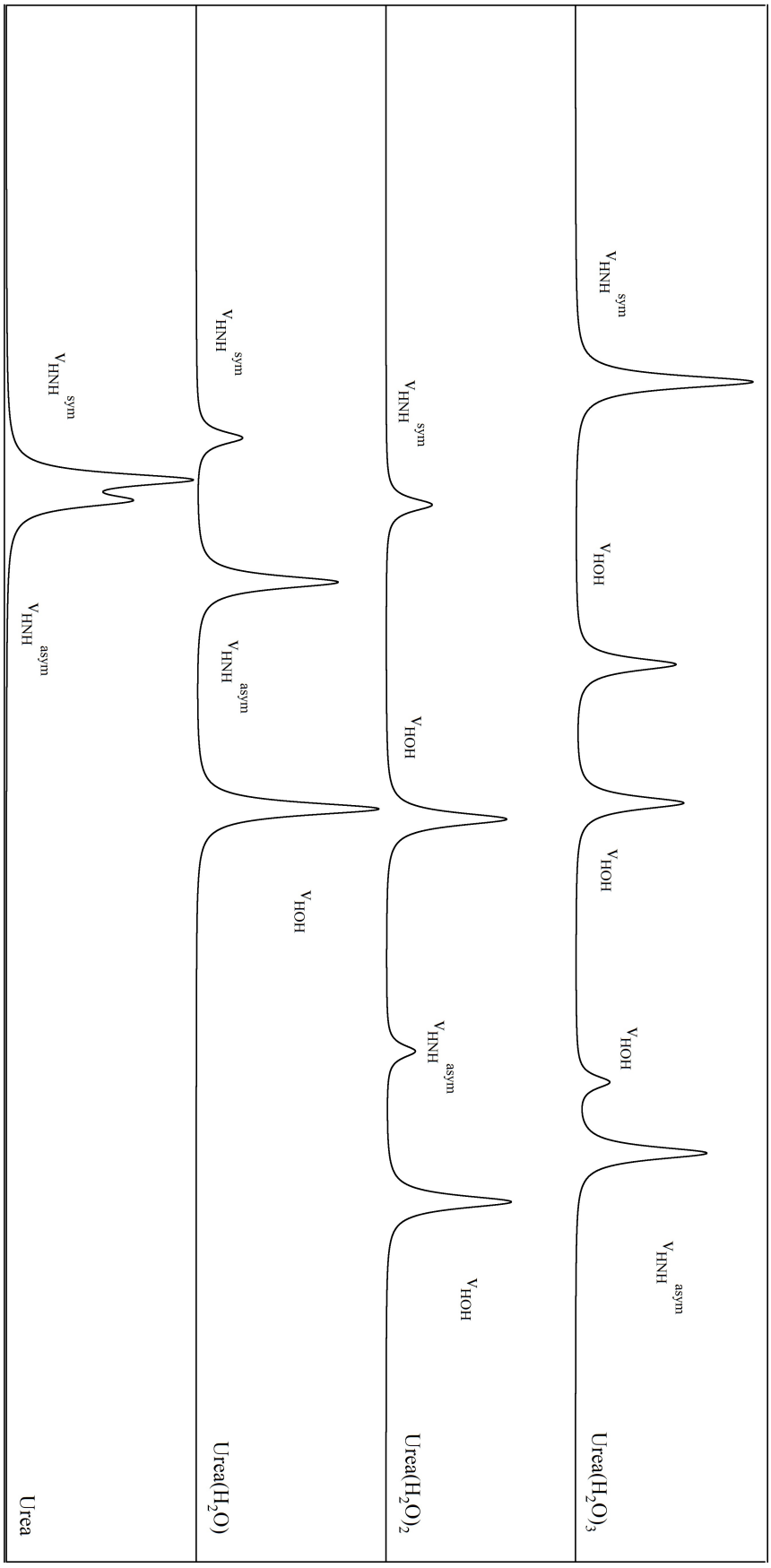

Figure 4.4.1: Simulatd Raman Spectra of Solvation of Urea

In Figure 4.4.1, theoretical solvation of urea was examined using lowest energy structures from each level of hydration. High resolution was used so that symmetric and asymmetric HNH urea bends and HOH water bends could easily be distinguished. From this figure, it is clear that water vibrational modes "split the symmetry" of the urea bending modes. In the presence of increasing water molecules, the HNH symmetric bending mode of urea actually decreases in energy (red shifts), while the HNH asymmetric bending mode blue shifts. Therefore, if hydration of urea causes a red shift of the HNH symmetric bending mode of urea, the blue shift of this mode in the presence of water and TMAO is most likely caused by the presence of TMAO. Furthermore, if water has no impact on the blue shift seen in experiment, the blue shift should be observed between a theoretical Raman spectrum of urea, alone, and a theoretical Raman spectrum of urea with TMAO. Figure 4.4.2 compares these two theoretical spectra.

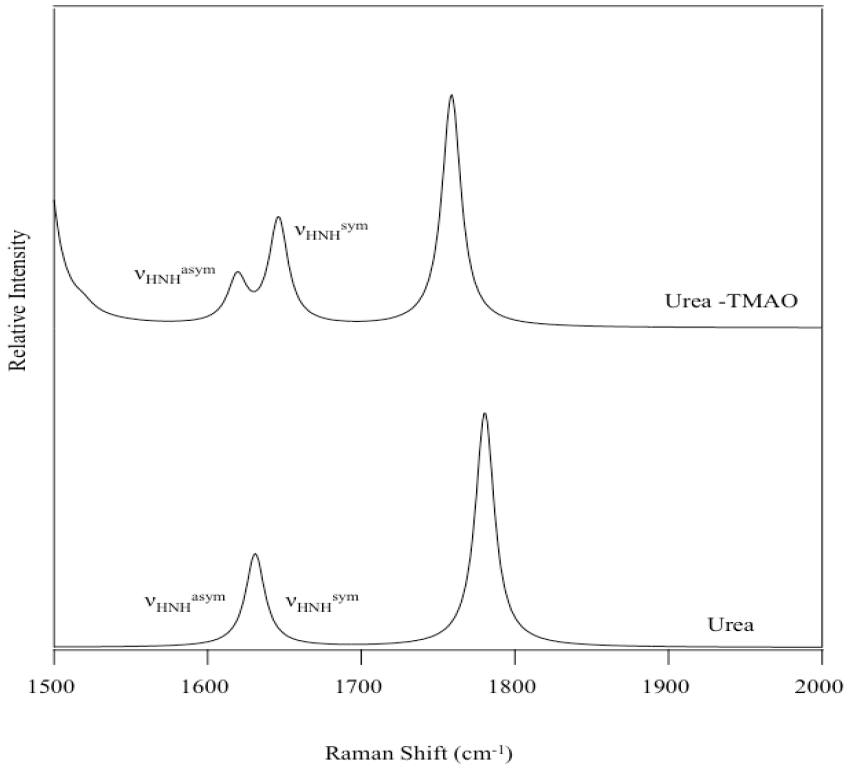

Figure 4.4.2: Simulated Raman Spectra Showing Blue Shift of urea symmetric bend caused by presence of TMAO

Figure 4.4.2 clearly shows a blue shift with a magnitude of about 15 cm^{-1} for the symmetric bend of urea in the presence of TMAO. The asymmetric bending mode red shifts by about 11 cm^{-1}. Structure B from Figure 4.2.6 was used in this comparison because it is believed to be a dimer structure found in experiment solutions based on previously discussed data. Interestingly, when the theoretical urea Raman spectrum and the Raman spectrum of structure A from Figure 4.2.6 are examined, the shifting directions of the two urea-bending modes are reversed. The symmetric urea-bending mode is redshifted by about 10 cm^{-1}, while the asymmetric urea-bending mode is blue shifted by 17 cm^{-1}.

4.5 Conclusions

In this experiment, the mechanism of TMAO's counteraction on urea is explored. Experimental Raman spectra of saturated TMAO and saturated urea were obtained from previous lab members' work. Raman spectroscopy was used to find Raman vibrational frequencies of a saturated solution of TMAO-urea dimers in water. Comparison of these three experimental spectra showed that only one vibration mode shifted significantly from saturated solutions of single osmolytes to saturated solutions of the dimer (Figure 4.1.9).

Theoretical calculations were carried out using Gaussian09. Urea-water optimized structures were created by increasing solvation of urea. The theoretical structures at lowest energy contained preferential spots where waters interacted with urea (pockets on either side of carbonyl oxygen and between amine groups of urea). Surprisingly, a water ring urea structure, with waters hydrogen bonding with each other, had a less stable

energy than three waters hydrogen bonding to urea spots. This data should be explored more fully as possible evidence that urea acts as a protein denaturant by destabilizing hydrogen bonding water networks.

Dimer structures involving both TMAO and urea were optimized theoretically with increasing water molecules. The symmetric urea bending mode of these structures' spectra were compared to symmetric urea bending modes of similar urea water structures' Raman spectra. Most theoretical dimer spectra contained blue shifted symmetric bending modes, consistent with experimental data. Simulating the addition of a TMAO molecule to a three water-urea structure produced a Raman blue shift. Furthermore, when TMAO replaced a water molecule (Figure 4.2.11 and Figure 4.2.12), a Raman blue shift was also observed. Interestingly, in Figure 4.2.12, the mode that is blue shifted is the asymmetric urea-bending mode not the symmetric bending mode. Finally, other possible causes of the experimental blue shift were studied. Through Raman spectra, theoretical increasing solvation of urea from zero to three water molecules caused a red shift in urea's symmetric bending mode, refuting the possibility that urea-water interaction could have caused the experimental blue shift (Figure 4.4.1). In Figure 4.4.2, the addition of TMAO to urea without any water molecules present caused a spectral blue shift similar to that found in experimental spectra. The experimental finding of a blue shifted urea symmetric bending mode in the presence of TMAO supports the hypothesis that TMAO counteract urea's denaturation by interacting directly with urea. This experimental shift is validated by optimized structures and theoretical Raman spectral shifts.

1. Nelson, D. L.; Cox, M. M., *Lehninger Principles of Biochemistry*. 5 ed.; W. H. Freeman: 2008; p 1100. 978-0716771081
2. Garcia-Perez, A., Importance of organic osmolytes for osmoregulation by renal medullary cells. *Hypertension: Journal of the American Heart Association* **1990,** *16*, 7. 10.1161/01.HYP.16.6.595
3. Wei, H., Effects of Urea, Tetramethyl Urea, and Trimethylamine N-Oxide on Aqueous Solution Structure and Solvation of Protein Backbones: A Molecular Dynamics Simulation Study. *Journal of Physical Chemistry* **2010,** *114* (1), 11. 10.1021/jp9084926
4. Cuellar, K. A.; Munroe, K. L.; Magers, D. H.; Hammer, N. I., Noncovalent interactions in microsolvated networks of trimethylamine N-oxide. *The journal of physical chemistry. B* **2014,** *118* (2), 449-59. 10.1021/jp408659n
5. Silverstein, T. P., The Real Reason Why Oil and Water Don't Mix. *Journal of Chemical Education* **1998,** *75* (1), 2. 10.1021/ed075p116
6. Sherwood, L., *Human Physiology: From Cells to Systems.* Brooks/Cole, Cengage Learning: Belmont, CA, 2013. 9781111577438
7. Sigma-Aldrich Amino Acids Reference Chart. http://www.sigmaaldrich.com/life-science/metabolomics/learning-center/amino-acid-reference-chart.html (accessed April 3).
8. Spolar, R. S.; Ha, J.-H.; Record Jr., M. T., Hydrophobic effect in protein folding and other noncovalent processes involving proteins. *Proc. Natl. Acad. Sci.* **1989,** *86*, 3.
9. Yancey, P. H., Organic osmolytes as compatible, metabolic and counteracting cytoprotectants in high osmolarity and other stresses. *J Exp Biol* **2005,** *208* (Pt 15), 2819-30. 10.1242/jeb.01730
10. Bolen, D. W., Protein Stabilization by Naturally Occurring Osmolytes. *Methods in Molecular Biology* **2001,** *168*. 10.1385/1-59259-193-0:017
11. Batchelor, J. D., Impact of Protein Denaturants and Stabilizers on Water Structure. *Journal of the American Chemical Society* **2004,** *126* (7), 3. 10.1021/ja039335h
12. Ma, J.; Pazos, I. M.; Gai, F., Microscopic insights into the protein-stabilizing effect of trimethylamine N-oxide (TMAO). *Proceedings of the National Academy of Sciences of the United States of America* **2014,** *111* (23), 8476-81. 10.1073/pnas.1403224111
13. Davis-Searles, P. R.; Saunders, A. J.; Erie, D. A.; Winzor, D. J.; Pielak, G. J., Interpreting the Effects of Small Uncharged Solutes on Protein-Folding Equilibria. *Annual Review of Biophysics and Molecular Structure* **2001**, 35. 10.1146/annurev.biophys.30.1.271
14. Kuffel, A.; Zielkiewicz, J., The hydrogen bond network structure within the hydration shell around simple osmolytes: urea, tetramethylurea, and trimethylamine-N-oxide, investigated using both a fixed charge and a polarizable water model. *The Journal of chemical physics* **2010,** *133* (3), 035102. 10.1063/1.3464768
15. Panuszko, A.; Bruz´dziak, P.; Zielkiewicz, J.; Wyrzykowski, D.; Stangret, J., Effects of Urea and Trimethylamine-N-oxide on the Properties of Water and the Secondary
Structure of Hen Egg White Lysozyme. *Journal of Physical Chemistry* **2009,** *113*, 12. 10.1021/jp904001m

16. Bennion, B. J.; Daggett, V., The molecular basis for the chemical denaturation of proteins by urea. *Proceedings of the National Academy of Sciences of the United States of America* **2003,** *100* (9), 5142-7. 10.1073/pnas.0930122100
17. Wang, A.; Bolen, D. W., A Naturally Occuring Protective System in Urea-Rich Cells: Mechanism of Osmolyte Protection of Proteins against Urea Denaturation. *Biochemistry* **1997,** *36* (30), 7. 10.1021/bi970247h
18. Qu, Y.; Bolen, D. W., Hydrogen Exchange Kinects of RNase A and the Urea:TMAO Paradigm. *Biochemistry* **2003,** *42* (19), 12. 10.1021/bi0206457
19. Meersman, F.; Bowron, D.; Soper, A. K.; Koch, M. H., Counteraction of urea by trimethylamine N-oxide is due to direct interaction. *Biophysical journal* **2009,** *97* (9), 2559-66. 10.1016/j.bpj.2009.08.017
20. Skelly Frame, E. M.; Frame, G.; Robinson, J. W., *Undergraduate Instrumental Analysis*. 7th Edition ed.; Francis and Taylor Group, LLC: 2014. 978-1420061352
21. Engel, T.; Reid, P., *Physical Chemistry*. 3rd ed.; Pearson Education, Inc.: Glenview, IL, 2012. 978-0321812001
22. Jenson, J. H., *Molecular Modeling Basics*. 1st ed.; Taylor & Francis: Boca Raton, FL, 2010. 978-1420075267
23. Nicholson, A. T. Raman Spectroscopic and Computational Analysis of the Effects of Non-Covalent Interactions on DMSO. University of Mississippi, 2014.
24. Frisch, M. J.; Trucks, G. W.; Schlegel, H. B.; Scuseria, G. E.; Robb, M. A.; Cheeseman, J. R.; Scalmani, G.; Barone, V.; Mennucci, B.; Petersson, G. A.; Nakatsuji, H.; Caricato, M.; Li, X.; Hratchian, H. P.; Izmaylov, A. F.; Bloino, J.; Zheng, G.; Sonnenberg, J. L.; Hada, M.; Ehara, M.; Toyota, K.; Fukuda, R.; Hasegawa, J.; Ishida, M.; Nakajima, T.; Honda, Y.; Kitao, O.; Nakai, H.; Vreven, T.; Montgomery Jr., J. A.; Peralta, J. E.; Ogliaro, F.; Bearpark, M. J.; Heyd, J.; Brothers, E. N.; Kudin, K. N.; Staroverov, V. N.; Kobayashi, R.; Normand, J.; Raghavachari, K.; Rendell, A. P.; Burant, J. C.; Iyengar, S. S.; Tomasi, J.; Cossi, M.; Rega, N.; Millam, N. J.; Klene, M.; Knox, J. E.; Cross, J. B.; Bakken, V.; Adamo, C.; Jaramillo, J.; Gomperts, R.; Stratmann, R. E.; Yazyev, O.; Austin, A. J.; Cammi, R.; Pomelli, C.; Ochterski, J. W.; Martin, R. L.; Morokuma, K.; Zakrzewski, V. G.; Voth, G. A.; Salvador, P.; Dannenberg, J. J.; Dapprich, S.; Daniels, A. D.; Farkas, Ö.; Foresman, J. B.; Ortiz, J. V.; Cioslowski, J.; Fox, D. J. *Gaussian 09*, Gaussian, Inc.: Wallingford, CT, USA, 2009.
25. Becke, A. D., Density-functional exchange-energy approximation with correct asymptotic behavior. *Physical Review A* **1988,** *38* (6), 3098-3100.
26. Becke, A. D., Density‐functional thermochemistry. III. The role of exact exchange. *The Journal of chemical physics* **1993,** *98* (7), 5648-5652. doi:http://dx.doi.org/10.1063/1.464913
27. Lee, C.; Yang, W.; Parr, R. G., Development of the Colle-Salvetti correlation-energy formula into a functional of the electron density. *Physical Review B* **1988,** *37* (2), 785-789.
28. McLean, A. D.; Chandler, G. S., Contracted Gaussian basis sets for molecular calculations. I. Second row atoms, Z=11–18. *The Journal of chemical physics* **1980,** *72* (10), 5639-5648. doi:http://dx.doi.org/10.1063/1.438980
29. Krishnan, R.; Binkley, J. S.; Seeger, R.; Pople, J. A., Self‐consistent molecular orbital methods. XX. A basis set for correlated wave functions. *The Journal of chemical physics* **1980,** *72* (1), 650-654. doi:http://dx.doi.org/10.1063/1.438955

30. Idrissi, A., Molecular structure and dynamics of liquids: aqueous urea solutions. *Spectrochimica Acta Part A: Molecular and Biomolecular Spectroscopy* **2005,** *61* (1–2), 1-17. http://dx.doi.org/10.1016/j.saa.2004.02.039